Land aerosol retrieval algorithm update for the MERIS 4th reprocessing

(Algorithm Theoretical Basis Document)

Didier RAMON [(1)] ***Mathieu COMPIEGNE*** [(1)] ***and Richard SANTER*** [(2)]

(1) HYGEOS, Euratechnologies, 165 Avenue de Bretagne, 59000 Lille, France
(2) Université du Littoral, Côte d'Opale, 1, place de l'Yser - BP 1022 - 59375 Dunkerque, France

21/11/2016

v 1.0

Issue	Date	Modified Items / Reason for Change
0.1	26.06.2014	First version issue 0.1
0.2	02.09.2014	Add a second BRDF model without any reference to DDV, Add a preliminary validation. Rename it ATBD
0.9	18.12.2014	Describe first BRDF LUT processing procedure
0.91	28.01.2015	Describe Kernels integrals LUT and show and example of LARS BRDF computation from LUTS
1.0	21.11.2016	Remove outdated paragraphs, add validation results and annexes

Acronyms

ARVI	Atmospheric Resistant Vegetation Index
NDVI	Normalized Difference Vegetation Index
AOT	Aerosol Optical Thickness
ATBD	Algorithm Theoretical Basic Document
BRDF	Bidirectional Reflectance Distribution Function
BRF	Bidirectional Reflectance Function
CCI	Climate Change Initiative
DDV	Dense Dark Vegetation
ESA	European Space Agency
LARS	Land Aerosol Remote Sensing
LUT	Look Up Table
MERIS	MEdium Resolution Imaging Spectrometer
MEGS	MERIS Ground Segment
MODIS	Moderate Resolution Imaging Spectroradiometer
POLDER	POLarization and Directionality of Earth Reflectance
SAM	Standard Aerosol Model
TOA	Top Of Atmosphere
BOA	Bottom of Atmosphere
WSA	White Sky Albedo
BSA	Black Sky Albedo
CMG	Climate Modeling Grid
AERONET	Aerosol Robotic NETwork

Table of Content

1 introduction

This document describes several evolutions of the MERIS aerosol retrieval algorithm over land that are proposed to be included into the 4th MERIS reprocessing.

1.1 Reference Documents

[RD1] Santer, R., Carrere, V., Dubuisson, P. and Roger, J. C., (1999), Atmospheric correction over land for MERIS. *International Journal of Remote Sensing*, **20**, pp. 1819-1840.

[RD2] Santer, R. and D. Ramon, (2011), MERIS aerosol remote sensing over land, Algorithm Theoretical Basis Document No 2.15 v5.0 of 12/07/2011, available at : https://earth.esa.int/instruments/meris/atbd/atbd_2.15.pdf

[RD3] Ramon, D. and R. Santer, (2000), Atmospheric corrections over land : correction of directional effects over DDV, Algorithm Theoretical Basis Document No 2.19 v4.1 of 18/02/2000, available at : https://earth.esa.int/instruments/meris/atbd/atbd_2_19.pdf

[RD4] MERIS level 2 Detailed Processing Model v8.0b of 24/06/2011 (PO-TN-MEL-GS-0006), available at : https://earth.esa.int/pub/ESA_DOC/ENVISAT/MERIS/MERIS-DPM-L2-i8r0B.pdf

[RD5] Zagolski, F., Specification of the scientific contents of the MERIS level-1b & 2 auxiliary data products (PO-RS-PAR-GS-0002) v3.c of 27/02/2011, available at : https://earth.esa.int/instruments/meris/rfm/PO-RS-PAR-GS-0002-3C-Prod_Spec.pdf

[RD6] Santer R., Ramon D., Vidot J., Dilligeard E., (2007), A Surface Reflectance Model for Aerosol Remote Sensing over Land, *International Journal of Remote Sensing*, Vol. **28,** Iss 3-4.

[RD7] Ramon D. and R. Santer, (2001), “Operational remote sensing of aerosols over land to account for directional effects”, *Applied Optics-LP*, **40**, 3060-3075.

[RD8] Ramon D. and R. Santer, (2008), “Validation of the aerosol product over land”, *Second MERIS-AATSR Workshop*, 22-26 September 2008, ESA-ESRIN, Frascati, Italy, 2008, presentation available at: http://earth.esa.int/workshops/meris_aatsr2008/participants/800/pres_800_Ramon.pdf

[RD9] Leroy, M., Bruniquel-Pinel, V., Hautecoeur, O., Bréon, F. M.,Baret, F., (1998), Corrections atmosphériques des données MERIS/ENVISAT: caractérisations de la BRDF de surfaces “sombres”, *European Space Agency final report*, 98 p.

[RD10] Bréon, F.-M., F. Maignan, M. Leroy, and I. Grant, (2002) “Analysis of hot spot directional signatures measured from space,” *J. Geophys. Res*., vol. **107**, no. D16, p. 4282.

[RD11] Maignan, F., F.-M. Bréon, and R. Lacaze, (2004), “Bidirectional reflectance of earth targets: Evaluation of analytical models using a large set of spaceborne measurements with emphasis on the hot spot”, *Remote Sens. Environ.*, vol. **90**, no. 2, pp. 210–220.

[RD12] Vermote, E., C.O. Justice and F.-M. Bréon, (2009), Towards a Generalized Approach for Correction of the BRDF Effect in MODIS Directional Reflectances , *IEEE Transactions on Geoscience and Remote Sensing*, Vol **47**, No 3, pp-898-908

[RD13] Strahler, A.H., J.P. Muller and MODIS Science Team, (2009), “MODIS Albedo/BRDF product : ATBD v5.0”, April 1999, available at : http://modis.gsfc.nasa.gov/data/atbd/atbd_mod09.pdf

[RD14] Fraser, R.S. and Y.J. Kaufman, (1985) « The Relative Importance of Aerosol Scattering and Absorption in Remote Sensing »,*IEEE Transactions on Geoscience and Remote Sensing*, Vol.GE-**23** ,Iss. 5, pp 625-633.

2 LARS Surface Reflectance

2.1 Status of the Land aerosol algorithm regarding surface reflectance estimation in the 3rd reprocessing

The concept of DDV is the basis of the aerosol retrieval strategy. The DDV is a vegetated dark target whose spectral properties depend on the biome type and season **[RD1]**. We have currently 11 biomes and 20 DDV models:

$$biome = g(lat, lon) \tag{2.1}$$

$$DDV = f(biome, month) \tag{2.2}$$

The initial DDV spectral BRDF is characterised at discrete angles from POLDER measurements **[RD9]**. They are fitted using Hapke's model **[RD3]** to enable computations in any direction and thus derived secondary LUT's such as ARVI thresholds and DDV -atmosphere coupling terms **[RD5], [RD7]**

$$\{\rho_{DDV}^{ijk}, \theta_s^i, \theta_v^j, \varphi^k | i, j, k\} \xrightarrow{\text{Hapke model}} \rho_{DDV}(\theta_s, \theta_v, \varphi), a_{DDV} \xrightarrow{RTC} ARVI_{DDV}^{TOA}(\theta_s, \theta_v, \varphi) \tag{2.3}$$

In order to deal with brighter target, the concept of LARS was introduced in **[RD6]**. The BRDF of the LARS target is now a function of the difference between the observed ARVI and the ARVI of DDV, ΔARVI, these quantities being taken at the TOA, for the particular observation geometry and for the current DDV model:

$$\Delta ARVI_{LARS}^{TOA}(\theta_s, \theta_v, \varphi) = ARVI_{LARS}^{TOA}(\theta_s, \theta_v, \varphi) - ARVI_{DDV}^{TOA}(\theta_s, \theta_v, \varphi) \tag{2.4}$$

After correcting the DDV BRDF by a scaling factor that depend on location and season to refine the initial only 20 values for DDV's albedo :

$$\rho_{DDV}^{norm}(\theta_s, \theta_v, \varphi, lat, lon, month) = \rho_{DDV}(\theta_s, \theta_v, \varphi) \cdot C^{norm}(lat, lon, month) \quad , \tag{2.5}$$

We apply a correction factor to the DDV BRDF to obtain the LARS BRDF. This correcting factor is a linear function of ΔARVI:

$$C_{LARS}^{ext}(\theta_s,\theta_v,\varphi,lat,lon,month)=\frac{\rho_{DDV}^{norm}(\theta_s,\theta_v,\varphi,lat,lon,month)+S^{ext}(lat,lon,month)\cdot\Delta ARVI^{TOA}(\theta_s,\theta_v,\varphi)}{\rho_{DDV}^{norm}(\theta_s,\theta_v,\varphi,lat,lon,month)} \quad (2.6)$$

$$\rho_{LARS}(\theta_s,\theta_v,\varphi,lat,lon,month)=\rho_{DDV}^{norm}(\theta_s,\theta_v,\varphi,lat,lon,month)+S^{ext}(lat,lon,month)\cdot\Delta ARVI^{TOA}(\theta_s,\theta_v,\varphi) \quad (2.7)$$

Although the LARS concept permits to obtain an aerosol product over land with a good cover without SWIR channels as for MODIS **[RD8]**, it was noticed during the 3rd reprocessing validation that the main limitation of the aerosol product, after cloud contamination issues, was the modelling of the LARS BRDF as described by Eq.2.7, whose shape is always similar to DDV's one.

2.2 State of the art for the correction of directional effects of surface reflectance

In **[RD10]**, **[RD11]**, most of Earth's targets BRDF are well modelled by a kernel driven model:

$$\rho_{LARS}(\theta_s,\theta_v,\varphi)=k_0+k_1F_1(\theta_s,\theta_v,\varphi)+k_2F_2(\theta_s,\theta_v,\varphi), \quad (2.8)$$

where the F1 kernel is the Ross Thick kernel corrected for the hot spot feature and the F2 kernel is the Li Sparse Reciprocal one. Following **[RD12]**, one can reformulate this equation as follows:

$$\rho_{LARS}(\theta_s,\theta_v,\varphi)=k_0[1+V(lat,lon,NDVI)F_1(\theta_s,\theta_v,\varphi)+R(lat,lon,NDVI)F_2(\theta_s,\theta_v,\varphi)] \quad (2.9)$$

This model is named VJB hereafter. The VJB model free parameters V (Volume scattering term within the canopy) and R (Surface scattering term related to surface roughness) are derived from Surface Reflectance time series coming from MODIS pluri annual CMG data (Climate Modeling Grid, regular grid 0.05° ~5600 m at equator, see for example Fig. 1). **They are linearly correlated with BOA NDVI** (see Fig. 2). This makes the link with the LARS concept. We can safely assume that they are also correlated with BOA and TOA ARVI. The only remaining unknown is $k_0(t)$.

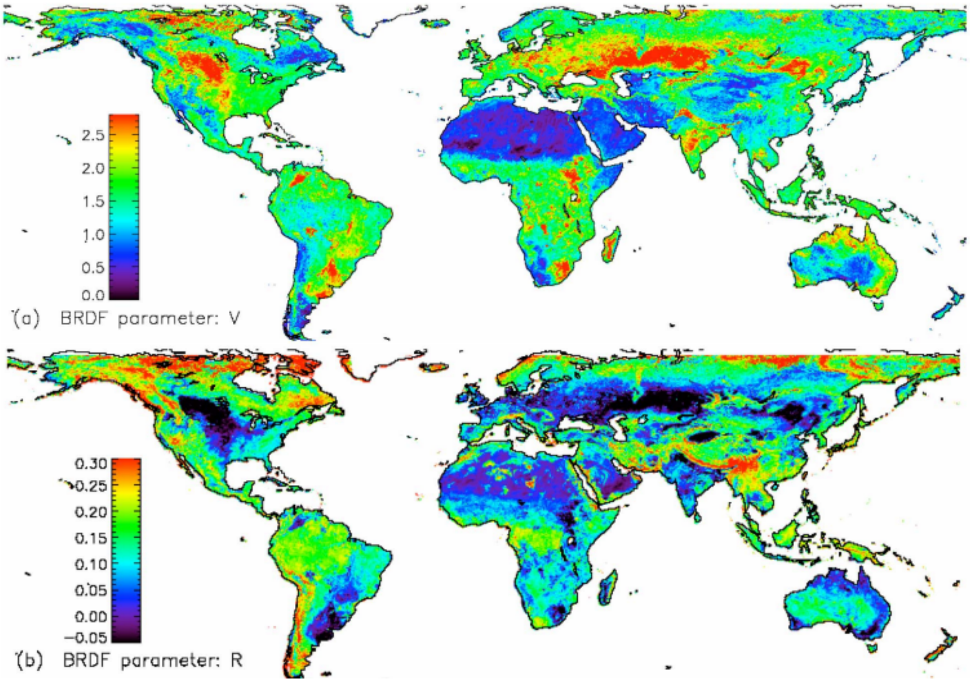

***Figure 1**: from **[RD12]**, R and V parameters derived from MODIS time series at 865 nm at the scale of 5600 m over the period 2000-2004 for the highest NDVI class.*

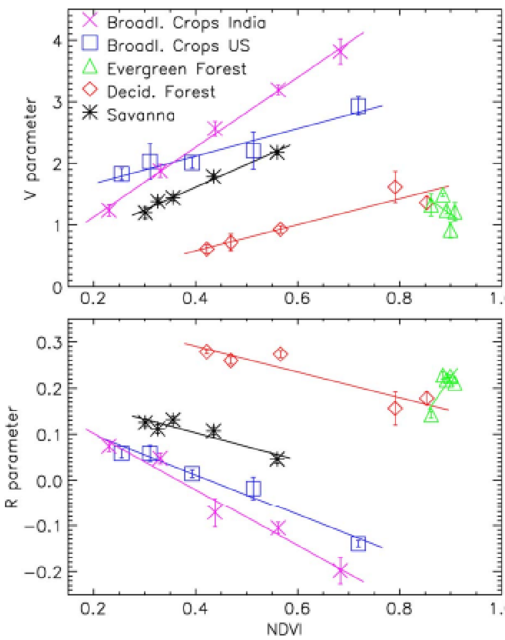

***Figure 2** from **[RD12]**, Variations of R and V parameters as a function of NDVI for several land cover*

2.3 New LARS BRDF Model

2.3.1 Model 1 : with DDV LUT's

Directional integration of the LARS BRDF is straightforward a kernel defined BRDF, one can derive LARS White Sky Albedo (**WSA**):

$$a_{LARS}=k_0\cdot[1+V(lat,lon,ARVI)A_1+R(lat,lon,ARVI)A_2] \tag{2.10}$$

With scalars A_1 and A_2 being the WSA of each kernel.

The above expression can be linked to the current definition of the LARS WSA :

$$a_{LARS}(lat,lon,month)=.\\ a_{DDV}^{norm}(lat,lon,month)+S^{ext}(lat,lon,month)\cdot\Delta ARVI^{TOA}(\theta_s,\theta_v,\varphi) \quad , \tag{2.11}$$

in order to derive the normalization term $k_0(t)$:

$$k_0(lat,lon,month,ARVI_{LARS}^{TOA}(\theta_s,\theta_v,\varphi))=.\\ \frac{a_{DDV}^{norm}(lat,lon,month)+S^{ext}(lat,lon,month)\cdot\Delta ARVI_{LARS}^{TOA}(\theta_s,\theta_v,\varphi)}{1+V(lat,lon,ARVI^{TOA}(\theta_s,\theta_v,\varphi))A_1+R(lat,lon,ARVI_{LARS}^{TOA}(\theta_s,\theta_v,\varphi))A_2} \tag{2.12}$$

We have now a LARS BRDF, Black Sky and White Sky Albedo characterization as a function of instantaneous TOA ARVI, lat, lon and month. It allows to perform all radiative transfer computations necessary for aerosol retrieval

2.3.1.1 Remarks:

After verification that this model recovers DDV for high ARVI, DDV BRDF LUT and DDV coupling terms with aerosols LUT become obsolete. Fig. 3 Shows one example of such fit.
However, DDV concept is old and corresponding LUT have never been updated. Therefore It is decided to get rid of any reference to DDV.

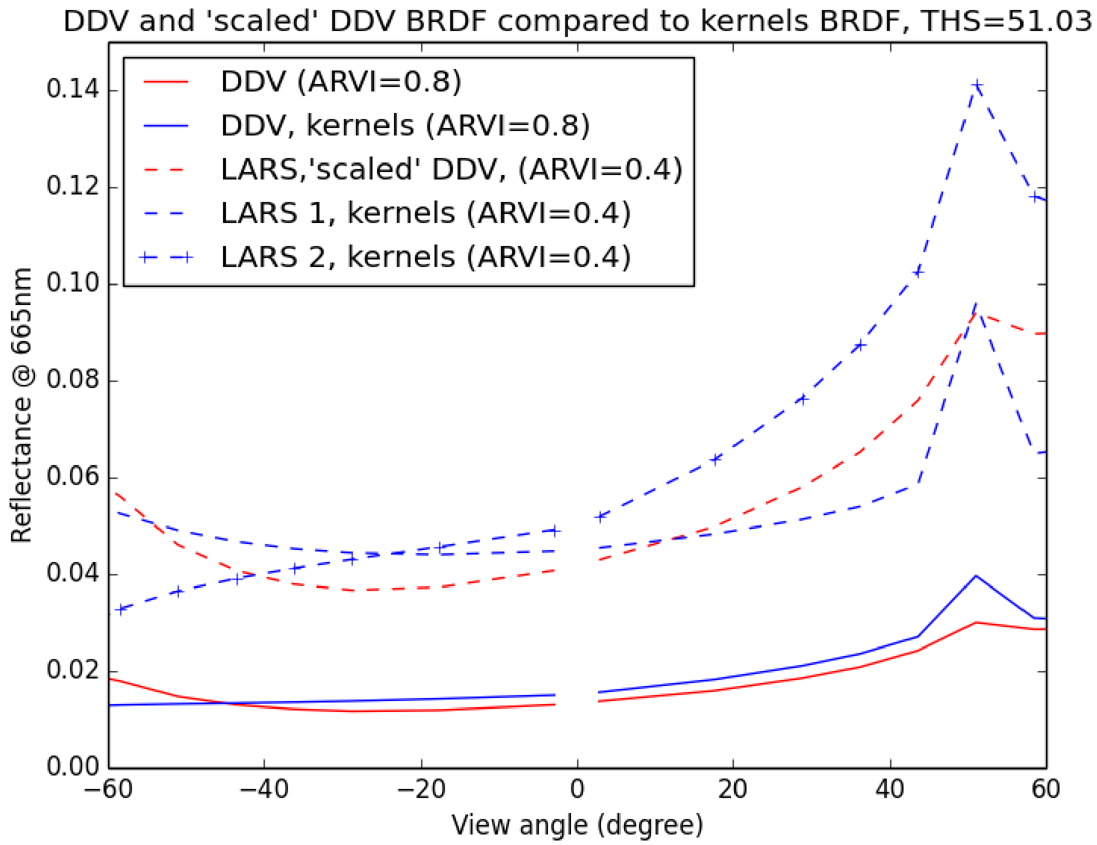

Figure 3*: Example of current LARS and kernel derived LARS BRDF*

2.3.2 Model 2 : no more DDV

Once the directional coefficients R and V have been derived for a given location, it is possible to correct for the directional effects any instantaneous surface reflectance measurement and obtain a directionally normalized reflectance $\tilde{\rho}$ with a particular geometry being taken as a reference, for example $\tilde{\theta}_s = 45°, \tilde{\theta}_v = 0°, \tilde{\varphi} = 0°$ as in [RD12]:

$$\tilde{\rho} = \rho(\theta_s, \theta_v, \varphi) \frac{1 + V\, F_1(45,0,0) + R\, F_2(45,0,0)}{1 + V\, F_1(\theta_s, \theta_v, \varphi) + R\, F_2(\theta_s, \theta_v, \varphi)} \tag{2.13}$$

Such a normalization is useful to reduce the noise in surface reflectance time series. An example is given in Fig. 4.

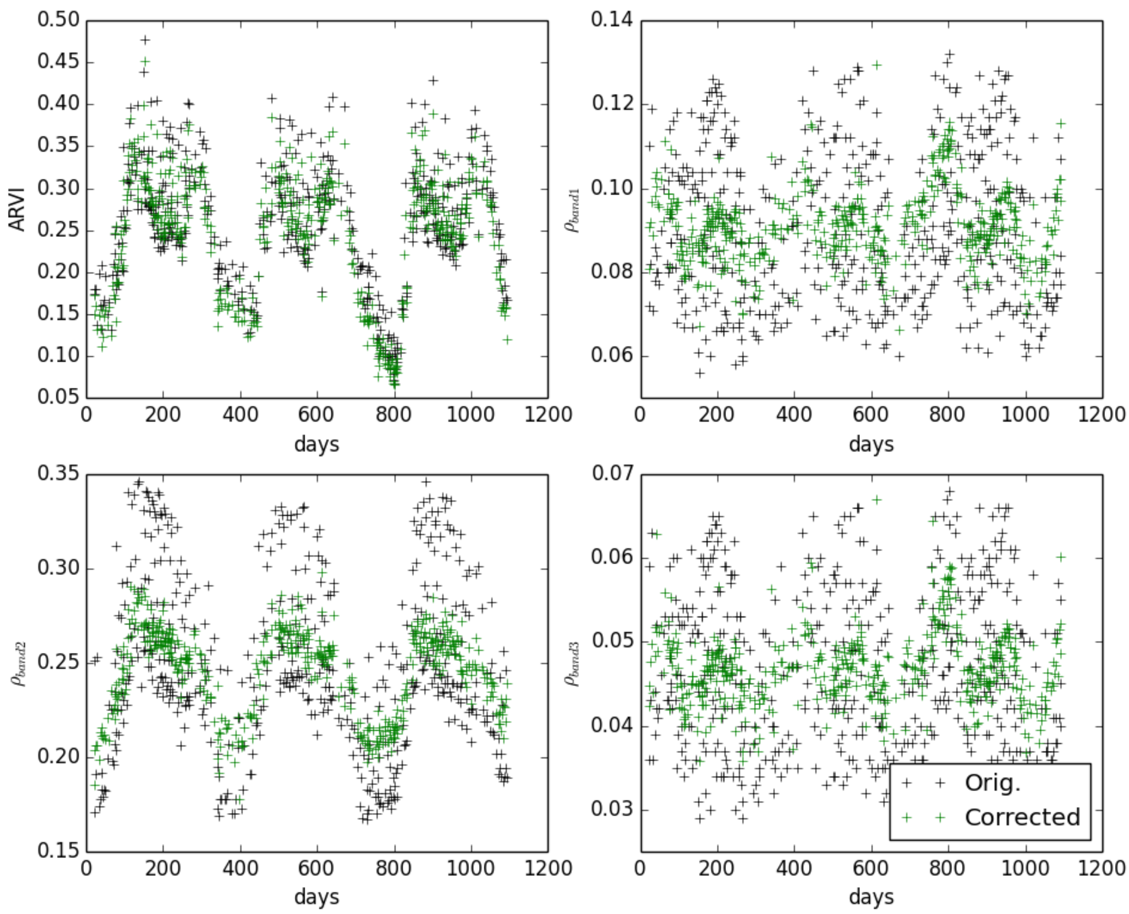

Figure 4*: Time series of Surface Reflectance (MODIS bands 1 (670nm) 2 (865nm) and 3 (470nm) from the MOD09CMG products from 2003-2005) and ARVI over the Avignon site, before and after normalization to the geometry θs=45° nadir view, using the R and V parameters previously retrieved.*

We can now directly connect the absolute value of the ARVI and the value of $\tilde{\rho}$. This can be done at the same spatial resolution as for the R and V parameters. Typical LARS linear regression for 0.05x0.05° boxes for each month can be obtained and neither reference to DDV ARVI's threshold nor DDV's albedo is necessary anymore (see an example Fig. 5):

$$\widetilde{\rho_{LARS}} = \alpha_{\tilde{\rho}}(lat, lon, \lambda) \cdot ARVI_{LARS}^{TOA} + \beta_{\tilde{\rho}}(lat, lon, \lambda) \quad (2.14)$$

The LARS BRDF is therefore:

$$\rho_{LARS}(\theta_s, \theta_v, \varphi) = \widetilde{\rho_{LARS}} \frac{1 + V F_1(\theta_s, \theta_v, \varphi) + R F_2(\theta_s, \theta_v, \varphi)}{1 + V F_1(45,0,0) + R F_2(45,0,0)} \quad (2.15)$$

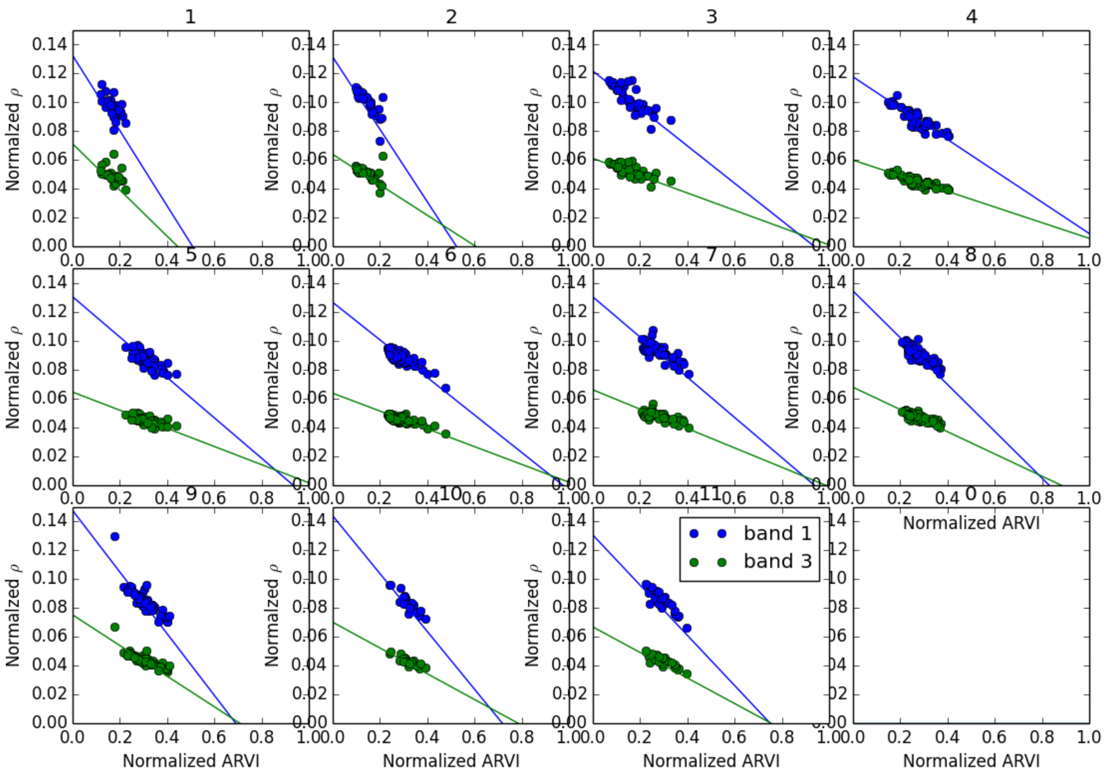

***Figure 5**: LARS linear regressions in MODIS band 1 (670nm) and 3 (470nm) derived from Normalized Surface Reflectance and ARVI, for each month and for the Avignon site.*

2.3.2.1 Remarks

- If necessary one could study whether a coarser resolution than 0.05 ° is still OK for the new LUT
- Dependence of R and V with ARVI can be certainly be linked theoretically to the dependence of LARS albedo with ARVI
- Deriving all BRDF parameters (Normalized reflectance and BRDF shape parameters R and V) from MERIS spectral surface reflectance time series could enhance consistency, but it requires some additional work. We tested this option with only MODIS data (see section 2.5)

2.4 Implementation of Model 2

2.4.1 Algorithm

For each pixel i,j with angles $\theta_s, \theta_v, \varphi$

New : Depending of latitude and longitude, obtain from nearest neighbor the linear regression parameters of the LARS BRDF shape factors R and V, and the reflectance for the normalization angle $\tilde{\rho}=\rho(\tilde{\theta}_s,0,0)$:

$$\alpha_R,\beta_R,\alpha_V,\beta_V,\alpha_{\tilde{\rho}},\beta_{\tilde{\rho}}=g(lat,lon,\lambda)\quad \text{On a regular grid whose size is } 1°. \tag{2.16}$$

New : Derive the LARS reflectance for the normalization angle

$$\widetilde{\rho_{LARS}}=\alpha_{\tilde{\rho}}(lat,lon,\lambda)\cdot ARVI_{LARS}^{TOA}+\beta_{\tilde{\rho}}(lat,lon,\lambda) \tag{2.17}$$

New : Compute R and V:

$$R,V=\alpha_{R,V}(lat,lon,\lambda)\cdot ARVI_{LARS}^{TOA}+\beta_{R,V}(lat,lon,\lambda) \tag{2.18}$$

Derive the normalization factor k_0 :

$$k_0=\frac{\widetilde{\rho_{LARS}}}{1+V\,F_1(\tilde{\theta}_s,0,0)+R\,F_2(\tilde{\theta}_s,0,0)} \tag{2.19}$$

The ground BRF is :

$$\rho_g=\rho_{LARS}(\theta_s,\theta_v,\varphi)=k_0\cdot[1+V\,F_1(\theta_s,\theta_v,\varphi)+R\,F_2(\theta_s,\theta_v,\varphi)] \tag{2.20}$$

and the ground Rayleigh coupling terms:

$$\overline{\rho_g^r}(\theta)=k_0\cdot[1+V\,\overline{F_1^r}(\theta)+R\,\overline{F_2^r}(\theta)], \tag{2.21}$$

with :

$$\overline{F_{1,2}}^r(\theta)=\frac{1}{\pi}\int_0^1\int_0^{2\pi}\mu\,F_{1,2}(\mu,\theta,\varphi)\,d\mu\,d\varphi \tag{2.22}$$

And the ground aerosol coupling terms:

$$\overline{\rho_g^a}(\theta_s,\theta_v,\varphi,iaer)=k_0\cdot[1+V\,\overline{F_1^a}(\theta_s,\theta_v,\varphi,iaer)+R\,\overline{F_2^a}(\theta_s,\theta_v,\varphi,iaer)] \tag{2.23}$$

with :

$$\overline{F_{1,2}}^{\downarrow a}(\theta_s,\theta_v,\varphi)=\frac{\int_0^1\int_0^{2\pi}\mu\,p_a(\theta_s,\mu,\varphi)\,F_{1,2}(\mu,\theta_v,\varphi'-\varphi)\,d\mu\,d\varphi'}{\int_0^1\int_0^{2\pi}\mu\,p_a(\theta_s,\mu,\varphi')\,d\mu\,d\varphi'} \tag{2.24}$$

The ground WSA is derived from both kernel's WSA, A_1 and A_2:

$$a_g = k_0 \cdot [1 + V A_1 + R A_2] \quad (2.25)$$

$$A_{1,2} = \frac{2}{\pi} \int_0^1 \int_0^{2\pi} \int_0^1 \mu_s \mu F_{1,2}(\mu_s, \mu, \varphi) \, d\mu_s \, d\mu \, d\varphi \quad (2.26)$$

2.4.2 LUT's

2.4.2.1 Description

The new table is the VJB model parameters $\alpha_R, \beta_R, \alpha_V, \beta_V$ is derived at the scale of **0.5°** from the MODIS surface reflectance MOD09CMG collection 5 product for the period 2003-2007. Indeed no band shifting is required as directional behaviour of the surface reflectance doesn't vary sharply with wavelength. The MODIS products were filtered to remove `SHADOW, CLOUD, CIRRUS, ADJACENT_TO_CLOUD, SNOW and FIRE` classified pixels.

$\alpha_{\tilde{\rho}}, \beta_{\tilde{\rho}}$ are the slope and intercept of the LARS reflectance monthly linear regression, for a normalization angle $\bar{\theta}_s$ of 45° are derived from the same dataset and the same spatial resolution. It could have been derived from MERIS surface reflectance time series, but at the time of the current release (18.12.2014), no such dataset was available.

NetCDF4 BRDF LUT description

Dataset Name	**Variables**	**type**	**size**
ALBE	$\alpha_{\tilde{\rho}}, \beta_{\tilde{\rho}}$	float32	(NLAT, NLON, NCOEF, NLAMBDA, NMONTH)
BRDF	$\alpha_R, \beta_R, \alpha_V, \beta_V$	float32	(NLAT, NLON, NCOEF, NPARAM, NLAMBDA)
QC	Quality Control index	int	(NLAT, NLON, NMONTH)

```
NLAT =     360
NLON   =   720
NCOEF=     2   (linear fit, first the slope then the intercept)
NPARAM=    2   (first V then R)
NLAMBDA=   2   (first MERIS B7 then B2)
NMONTH=    12
```

the QC index is an internal indicator of the quality of the fits, built from a series of tests:

- Max. Rmse of the normalized LARS reflectance fit in the blue `TOL_BLUE:0.01`
- Max. Rmse of the normalized LARS reflectance fit in the red `TOL_RED :0.01`
- Max. Rmse of the R,V fit `TOL_RV : 0.1`
- Minimum number of points for a fit `NPTS_MIN : 5`

- Minimum amplitude of ARVI for a fit `DARVI_MIN : 0.15`
- Minimum ARVI for the upper limit of the ARVI amplitude `ARVI_MIN: 0`

It is complemented by other LUT's corresponding to the coupling terms between ground and atmosphere **[RD3][RD7]**. They are built from the angle integration of BRDF kernels F_1 and F_2 (Eqs. 2.22 and 2.24) and are replacing old LUT's robar_rg_LUT and robar_ag_LUT (LUT no 320 and 321, see **[RD5]**) (smooth functions of θ; a 3 order polynomial is sufficient see **[RD13],** pp15-16). We do not plan to change dramatically the format of these coupling terms LUT's. The only difference is that we replace the dimension corresponding to 20 DDV models by 2 different kernels.
The complexity of the new surface reflectance model is reduced compared to the current one.

Kernels integrals LUT description

Dataset Name	**Variables**	**type**	**size**
FRbar	$\overline{F_{1,2}}^{r}(\theta)$	float32	(NTHETA,NPARAM)
FAbar	$\overline{F_{1,2}}^{a}(\theta_s,\theta_v,\varphi)$	float32	(NTHETA,NTHETA,NPHI,NPARAM)
A1	A_1	float32	Scalar, val= +9.51090E-02
A2	A_2	float32	Scalar, val= -1.37720E+00

```
NTHETA =  90 (from 89° to 0° by step of 1°)
NPHI =    19 (from 0° to 180° by step of 10°)
NPARAM =  2  (first F1 then F2)
```

2.4.2.2 Example

We give hereafter an example for a European zone. Figure 6 shows the ALBE extraction for the X=79 and Y=393 geographical grid point. The regression in July for an ARVI of 0.5 gives the corresponding values: $\tilde{\rho}(665)=0{,}0565, \tilde{\rho}(443)=0{,}0290$

On Figure 7, the regressions of the BRDF gives the following values V(665)=1.3, V(443)=1.2,R(665)=0.22,R(443)=0.23

These LARS BRDF parameters yield the following LARS BRDF and coupling terms in Figure 8 for the principal plane and a SZA of 45°

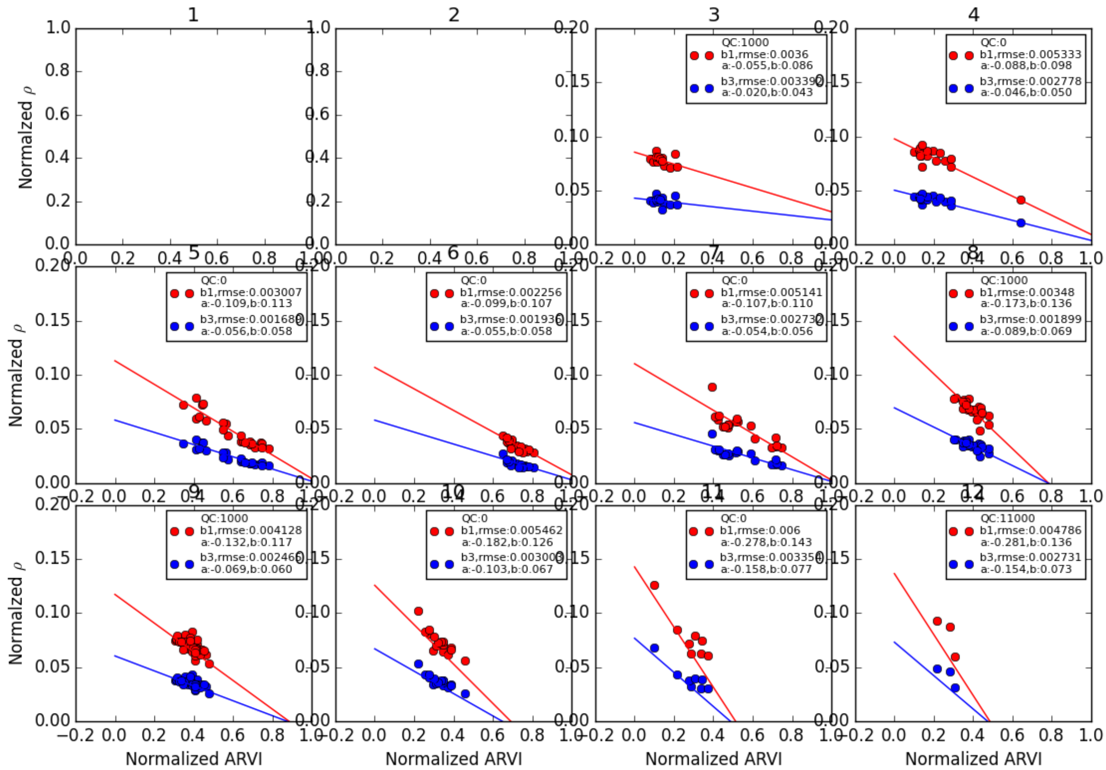

Figure 6: ALBE extraction for band 1 (670nm) and 3 (470nm) derived from Normalized Surface Reflectance and ARVI, for each month for a European zone

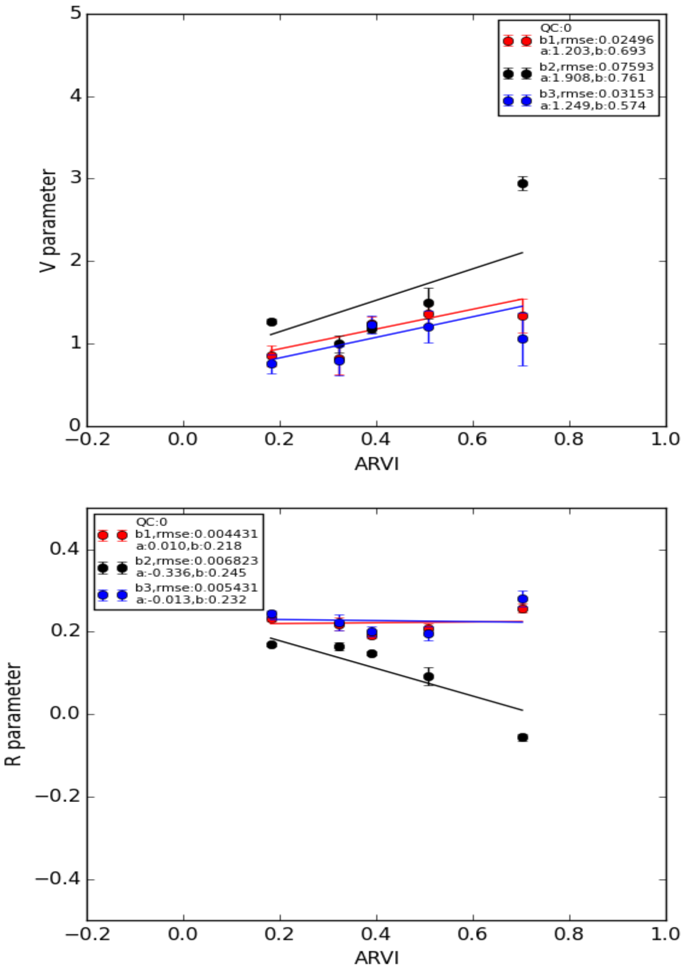

Figure 7: BRDF extraction for band 1 (670nm), band 2(865 nm) and 3 (470nm) derived from Normalized Surface Reflectance and ARVI, for the zone european zone of Fig 6

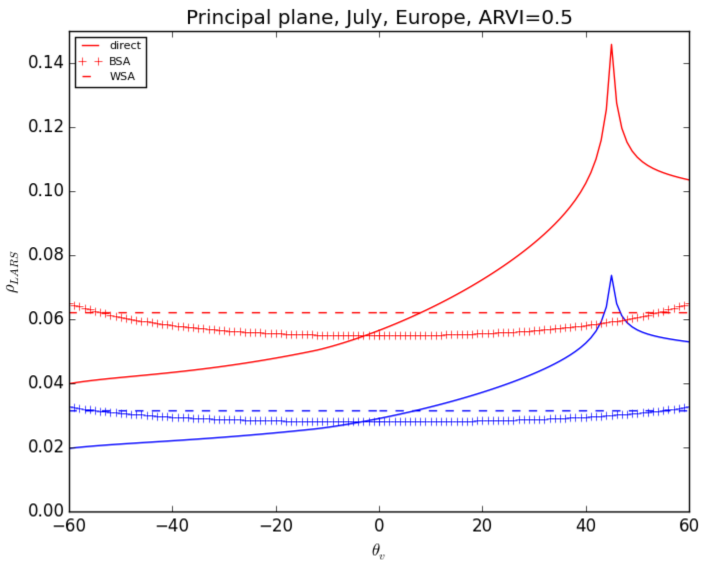

Figure 8: BRDF, Black sky albedo and White sky albedo of LARS

More spatialized examples are given in Annex 6.

2.5 Verification

We used the MODIS surface reflectance product MOD09CMG for all AERONET sites, for the period 2003-2005 at the native spatial resolution (0.05°) to compute the kernel based LARS BRDF model parameters (without DDV). Then we analyzed the AEROLAND database acquired over the AERONET sites, i.e. MERIS data coming from MEG8.1 over 10x10 RR super pixels for several months in 2008, and computed the following reflectances at 670 and 443 nm :

- current LARS reflectance
- kernel based LARS reflectance
- MERIS surface reflectance after aerosol correction using the AOT coming from AERONET and a continental aerosol model.

We applied also a filter on the MERIS AOT spatial standard deviation (<0.1) in order to reject cloud contaminated super pixels.
An example is given in Fig.9 for the Avignon site. Other examples are given in Annex 5

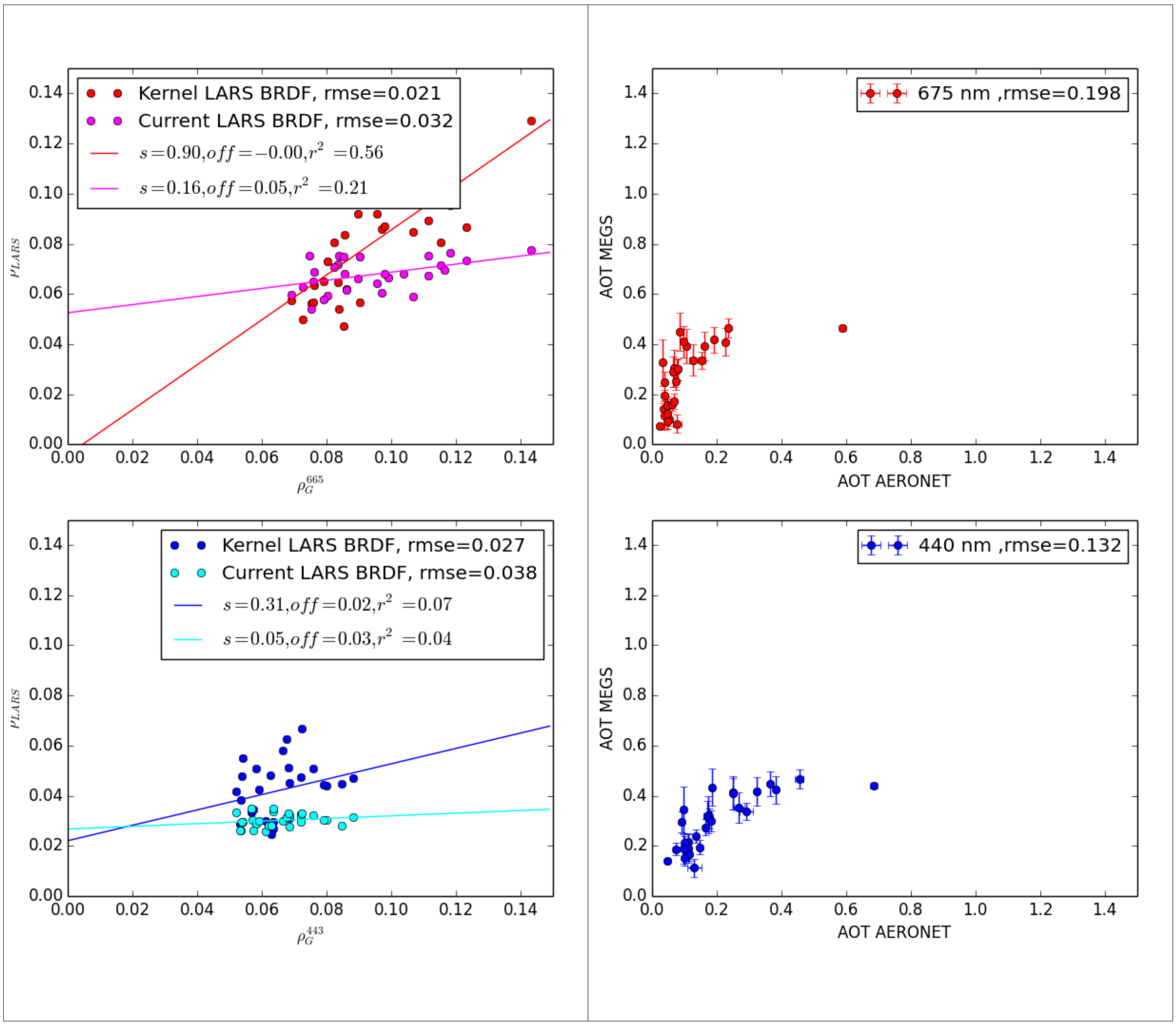

Figure 9: Surface reflectance at 665 nm and 443 nm derived from MERIS atmospherically corrected TOA reflectance using Aeronet aerosol information arounf the Avignon (43N,4E) site. It is compared to LARS predicted surface reflectance in the 3rd RP ("Current") and 4th RP ("Kernel"). We give also AOT retrieved from MEGS8.1 and Aeronet AOT.

3 Aerosol Model selection

3.1 Introduction

For the first processing, bands 1, 2 and 7 were used to retrieve the aerosol model. Because of the high Rayleigh contribution in band 1, this spectral band is no longer used. Since the third processing, the aerosol product retrieval is based on the use of bands 2 and 7 in order to retrieve the two aerosol parameters: the aerosol optical thickness (AOT) in one reference wavelength (550 nm) and the Angström coefficient α. Nevertheless, the algorithm was not changed. It is the objective of section 3.2 to indicate how to simplify the algorithm and to make it faster.

An accurate determination of α relies on the good knowledge of the LARS reflectance mainly in B7 where the vegetation is not as dark as in B2 (see section 2). A default value of α is used to derive the AOT. This aerosol model corresponds to α =1 and to non absorbing aerosol with a refractive index of 1.44. The aerosol climatology as provided by AERONET can propose a better choice of the default aerosol model as explained in section 3.3.

A better description of the surface reflectance of the LARS pixels, as foreseen, should improve the determination of α. We propose in section 3.4 how to take advantage of this.

3.2 Simplify the algorithm

3.2.1 3rd Reprocessing

We just described the section of the DPM **[RD4]** to be changed. It corresponds to:

(i) *Select band set (DPM 9-18)*

Select bands 2 & 7

(ii) *Retrieval of the MERIS TOA reflectance (after gaseous absorption: Rho_ng) in selected b (DPM 9-20) b=2 &7*

Loop on 26 aerosol types (`ia`=1 to 26)

Retrieval of the AOT for the 26 aerosol types AOT(B2,`ia`)

(iii) Determination of α in b=7. (to introduce)

If 2 bands, then compute directly α

If 3 bands, then linear regression to compute α

3.2.2 Modifications for 4th Reprocessing

We always select two bands b=2 and 7.

(a) In a loop on 26 aerosol types (`ia`=1 to 26); the 26 AOT's are determined in B2 as before. Then we use B7.

(b) First we compute the TOA for the N=26 aerosols, with:

(i) convert `AOT_550(ia)` in `AOT_B7` (*(2.6.17.4-4)*)

(ii)compute the Rho_ag (TOA after gaseous correction) in B7: `Rho_ag(ia)` *(2.6.17.3-50)*

(c) We select the aerosol type allowing retrieving `Rho_ng`. The predicted TOA in B7, `Rho_ag`, should decrease with `ia`. Indeed, in the red, the TOA signal for targets with albedo lower than 0.2 (this is always the case for LARS) increases monotonically with AOT for not too absorbing aerosol types (ωo >0.8) **[RD14]** and thus, for a given AOT at 550 the signal varies monotonically with the Junge exponent.

Moreover, if we believe that we mostly have small aerosols over land then we decrease from `ia`=26 to 1 to stop when `Rho_ag` (`ia`)>=`Rho_ng` and do the linear interpolations when the convergence exists. We have:
(i) if `Rho_ag` (`ia`=26)>`Rho_ng`; we do loop on `ia` and abandon the α retrieval. Flag and default values as for MEGS8.1
(ii) when `Rho_ag` (`ia`)>=`Rho_ng` , we stop the `ia` loop and retain `iat`=`ia`
(v) If the condition `Rho_ag` (`ia`)<=`Rho_ng` is not reached for `ia`=0, flag and default values as for MEGS8.1
(d) Interpolation to get α
We do a linear interpolation to compute α between 0.1*`iat` and 0.1*(`iat`-1)

$$\alpha=0.1*(iat-1+(Rho\_ng-Rho\_ag(iat))/(Rho\_ag(iat)-Rho\_ag(iat-1))$$

3.3 Default aerosol type selection

3.3.1 3rd Reprocessing

The aerosol remote sensing over land is challenging. Most of the LARS algorithms provide only one aerosol parameter: `AOT_550` based on the selected aerosol type. For MERIS, the determination of the AOT is done for the June model with α=1 (`ia`=16): *DPM 9.20 (2.6.17.3-18)*
The selection of the aerosol family (here through three values of the refractive index) was done with the `Aerclim_LUT`[lat,lon,month,k] with: lat : 0,180 by 1deg, lon : 360 by 1 deg: *DPM 9.12*. By default, k=2 (refractive index=1.44) *DPM 9.12 (2.6.17.1-1)*

3.3.2 Modifications for 4th Reprocessing

A climatology of the default aerosol model is a plus with as possible option:
(i) Based on the fact that k is everywhere and always equal to 2, the `Aerclim_LUT` is no longer used. We use the `Aerclim_LUT` to define the default aerosol model with k=1 to 26. AERONET and the monthly statistic provide the ingredients of this LUT.
(ii) `Aerclim_LUT` is used to define the default aerosol model `iac` to compute the AOT_440 and then the `AOT_550`.

3.3.3 Generation of the Aerclim_LUT

3.3.3.1 LUT from MODIS Level 3 data

We used MODIS Aqua Land Aerosol Monthly L3 product on th CMG grid (1x1°), MYD08_M3 collection 6.

The dataset chosen is '`Deep_Blue_Angstrom_Exponent_Land_Mean_Mean`', and is averaged from year 2003 to 2012.

<u>Key references</u>:

Hsu, N. C., S. C. Tsay, M. D. King, and J. R. Herman (2004), Aerosol properties over bright-reflecting source regions, IEEE Trans. Geosci. Remote Sens., 42, 557–569

Hsu, N. C., S. C. Tsay, M. D. King, and J. R. Herman (2006), Deep blue retrievals of Asian aerosol properties during ACE-Asia, IEEE Trans. Geosci. Remote Sens., 44, 3180–3195

Hsu, N. C., M.-J. Jeong, C. Bettenhausen, A. M. Sayer, R. Hansell, C. S. Seftor, J. Huang, and S.-C. Tsay (2013), Enhanced Deep Blue aerosol retrieval algorithm: The second generation, J. Geophys. Res. Atmos., 118, 9296–9315, doi:10.1002/jgrd.50712

Sayer, A. M., N. C. Hsu, C. Bettenhausen, and M.-J. Jeong (2013), Validation and uncertainty estimates for MODIS Collection 6 “Deep Blue” aerosol data, J. Geophys. Res. Atmos., 118, 7864–7872, doi:10.1002/jgrd.50600

Links:

MODIS Atmospheres website: modis-atmos.gsfc.nasa.gov

NASA LAADS (data distribution) website: ladsweb.nascom.nasa.gov

MODIS Collection 6 on the NASA LAADS ftp server: ladsweb.nascom.nasa.gov/allData/6/

Procedure

- Do Monthly means for the perdiod 2003-2012
- Do yearly means for backup in case of lacking monthly means.
- Fill remaining gaps of the backup with avreage value of 1.5
- Rely Ansgtrom exponent with model number
  - there is 78 models with Angstrom coefficient from 0 to 2.5 by step of 0.1, for three refractives indices 1.33, 1.44, 1.55. We keep only n=1.44

3.3.3.2 LUT Description

AeroClim LUT description

Dataset Name	Variables	type	size
`Aer. Model #`	Model index	`int`	`(NLAT,NLON, NMONTH)`

```
NLAT   =  180
NLON   =  360
NMONTH =  12
```

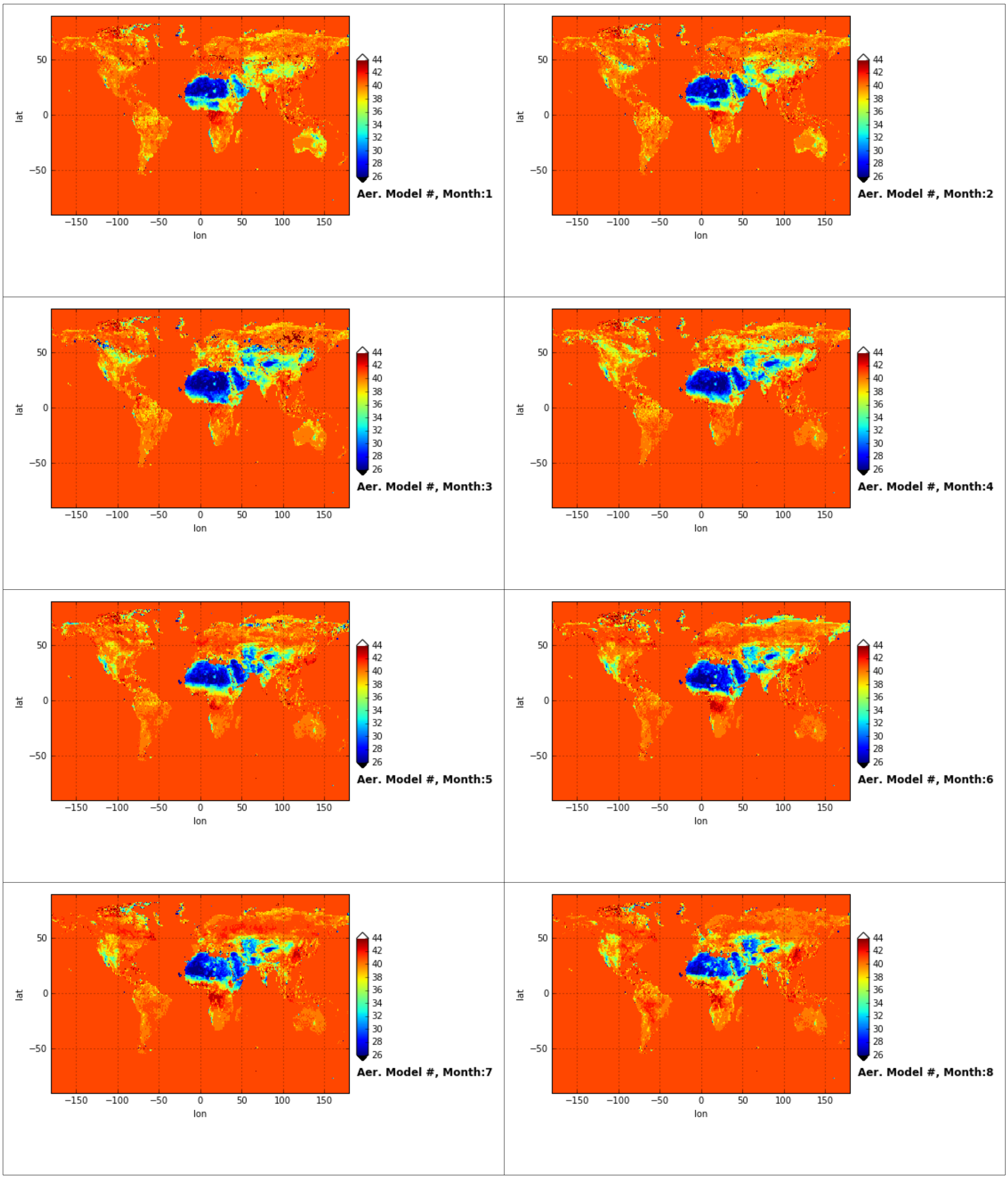

Aer. Model #, Month:1
Aer. Model #, Month:2
Aer. Model #, Month:3
Aer. Model #, Month:4
Aer. Model #, Month:5
Aer. Model #, Month:6
Aer. Model #, Month:7
Aer. Model #, Month:8
lat
lon

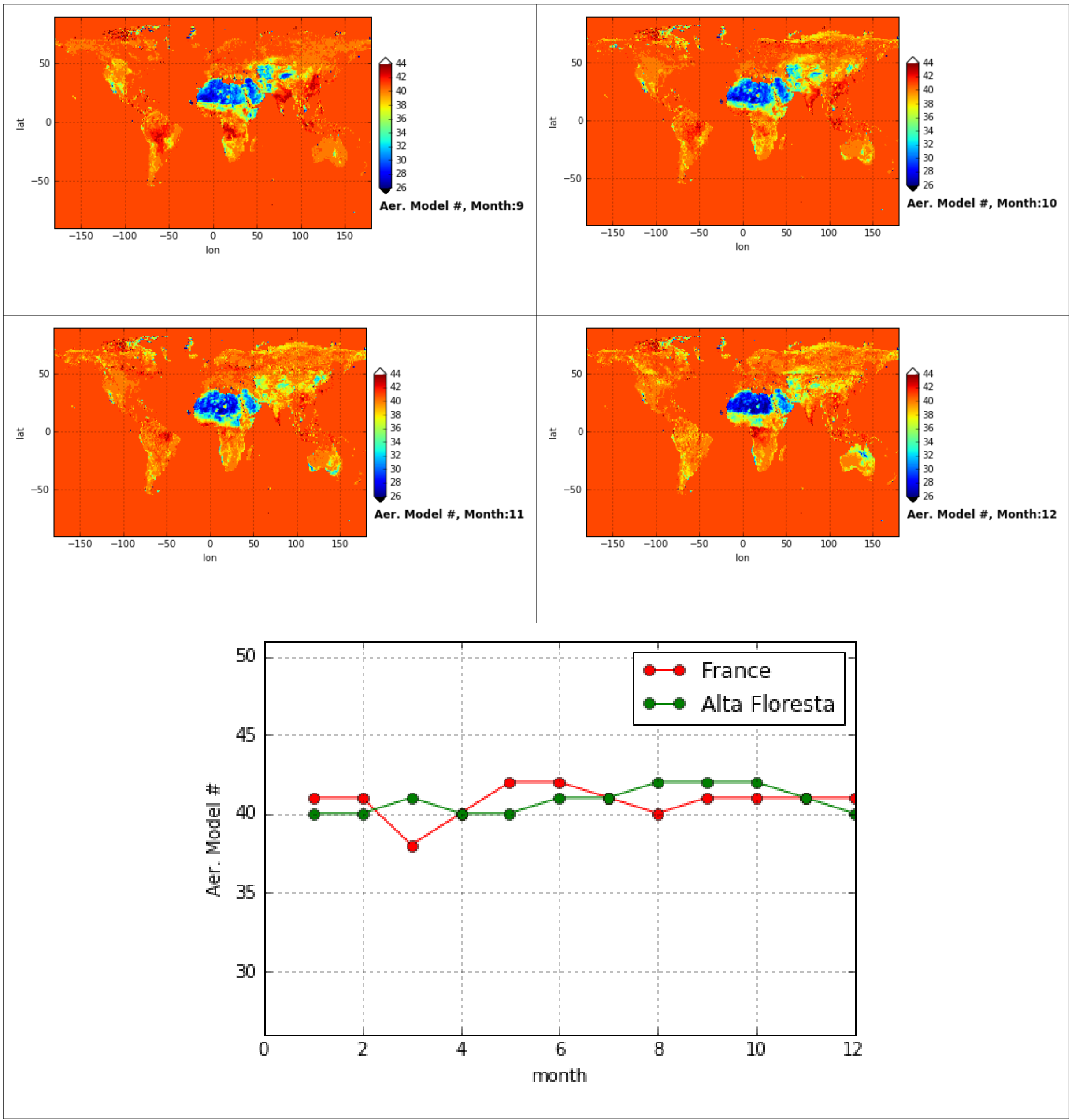

Figure 10: New Aerosol Climatology LUT (Aerosol model index as a function of location and month) and exampleq for Amazonian and European areas

3.4 Additional AOT at 550nm in the L2 product

3.4.1 Motivation

The introduction of a new LARS BDRF may potentially improve the retrieval of α. Therefore, it is suitable to propose the `AOT_550_alpha` as given by the retrieved aerosol type. The user will then have the choice between this `AOT_550_alpha` and the present

AOT_550. The recommendation is to use AOT_550_alpha if:
(i) AOT_550_alpha >0.05: for small aerosol abundances, the determination of α is inaccurate.
(ii) In a window of 8RRx8RR pixels (It corresponds approximately to the MODIS resolution of the daily aerosol product), we can rely on the mean value of α and therefore average the AOT_550 for the pixels at one r.m.s. in α.
The two above recommendations are relevant to generate a daily MERIS L3 aerosol product. More over the AOT_550_alpha and the AOT_550 can be used to convert all the AOT_555 in AOT_550_alpha _mean; the value for the mean α.

3.4.2 Modifications for 4th Reprocessing

AOT_550 is known for aerosol type iat and (iat-1) that is for α equal 0.1*iat and 0.1*(iat-1). AOT_550_alpha is know by linear interpolation between 0.1*iat and 0.1*(iat-1) on AOT_550(iat) and AOT_550(iat-1).
AOT_550_alpha Is included in the L2 product after AOT_550 after

4 Validation

4.1 Validation against AERONET data

ODESA with MEGS 8.1 (3rd RP) and MEGS 9.1 (4th RP) were parametrized in order to process L1B MERIS data in CSV_MERMAID mode with AERONET extractions for several sites and the whole MERIS archive. The extraction was done for 11x11 RR pixels boxes and the following parameters were extacted:

[A442, A442_err, ALPHA_L, ALTITUDE, AOPT_L, BRIGHT, CLOUD, COASTLINE, COSMETIC, DELTA_AZIMUTH, DETECTOR, DUPLICATED, GLINT_RISK, INVALID, L2FLAGS_L, LAND, LAND_OCEAN, LAT, LON, L_PCD_14, L_PCD_15, L_PCD_16, L_PCD_17, L_PCD_18, L_PCD_19, L_PCD_1_13, OZONE_ECMWF, PRESS_ECMWF, Q, RHO_GROUND_1, RHO_GROUND_2, RHO_GROUND_3, RHO_TOA_01, RHO_TOA_02, RHO_TOA_03, RHO_TOA_04, RHO_TOA_05, RHO_TOA_06,RHO_TOA_07, RHO_TOA_08, RHO_TOA_09, RHO_TOA_10, RHO_TOA_11, RHO_TOA_12, RHO_TOA_13, RHO_TOA_14, RHO_TOA_15, RH_ECMWF_01, RH_ECMWF_02, RH_ECMWF_03, RH_ECMWF_04, RH_ECMWF_05,RH_ECMWF_06, RH_ECMWF_07, RH_ECMWF_08, RH_ECMWF_09, RH_ECMWF_10, RH_ECMWF_11,RH_ECMWF_12, RH_ECMWF_13, RH_ECMWF_14, RH_ECMWF_15, RH_ECMWF_16, RH_ECMWF_17,RH_ECMWF_18, RH_ECMWF_19, RH_ECMWF_20, SCATT_ANGLE, SUN_AZIMUTH, SUN_ZENITH, SUSPECT, T442, T442_err, TAU_AER_L_02, TAU_AER_L_05, TAU_AER_L_07, T_ECMWF_01, T_ECMWF_02, T_ECMWF_03, T_ECMWF_04, T_ECMWF_05, T_ECMWF_06, T_ECMWF_07, T_ECMWF_08, T_ECMWF_09,T_ECMWF_10, T_ECMWF_11, T_ECMWF_12, T_ECMWF_13, T_ECMWF_14, T_ECMWF_15, T_ECMWF_16,T_ECMWF_17, T_ECMWF_18, T_ECMWF_19, T_ECMWF_20, VIEW_AZIMUTH, VIEW_ZENITH, WATER,WINDM, WINDU, WINDV, WV_ECMWF, thetas_IS]

the **CLOUD** mask was extended using the morphological operator **`dilate`** with a width of **10** pixels after tests with ACRI and the experienced gained during the CCI Aerosol project for which this value was used for the 3rd reprocessing aerosol product in order to minimize the cloud contamination. Within a 11x11 box, the mean and standard deviation of the Aerosol optical thicknesses and Angtsrom coefficient were computed. The matchups whose **standard deviation** of AOT exceeded **0.1** were discarded from the regression analysis. We didn' t apply any other selection criteria like for example the new “Q” field for “Quality” that is related to the darkness of the surface through the ARVI (Q=0 meaning a low ARVI, bright target, and Q>=8, is Dense Dark Vegetation), or the “QC” field in the LARS look up tables.

An example of the regression analysis is given in Figure 11, for the GSFC Aeronet site. In all plots the **AERONET** data are in the **`x`** axis where different **MEGS** outputs are given in the **`y`** axis:

- `TAU_AER_L_02`: Aerosol Optical Thickness at 442 nm derived jointly with the Aerosol Ansgtröm Coefficient, this is a new experimental output of MEG9.1.
- `T442` : Aerosol Optical Thickness at 442 nm derived using the new Aerosol Ansgtröm Coefficient climatology LUT. this is the standard output of MEG9.1
- `T442 (old AerClim)` : Aerosol Optical Thickness at 442 nm derived using the “old” (3rd RP) Aerosol Ansgtröm Coefficient climatology LUT. this is a test output of MEG9.1
- `A442`: Aerosol Angstrom Coefficient. this is the standard output of MEG9.1
- `ALPHA`: Aerosol Angstrom Coefficient. this is the standard output of MEG8.1
- `AOPT` : Aerosol Optical Thickness at 442 nm. this is a standard output of MEG8.1

The following regression parameters are given for each plot:

- R2: correlation coefficient
- N: number of points
- bias: mean(Y-X)
- reserr: residual error, std(Y-X)
- RMS: root mean square error : sum(((X-Y)/X)**2)/N

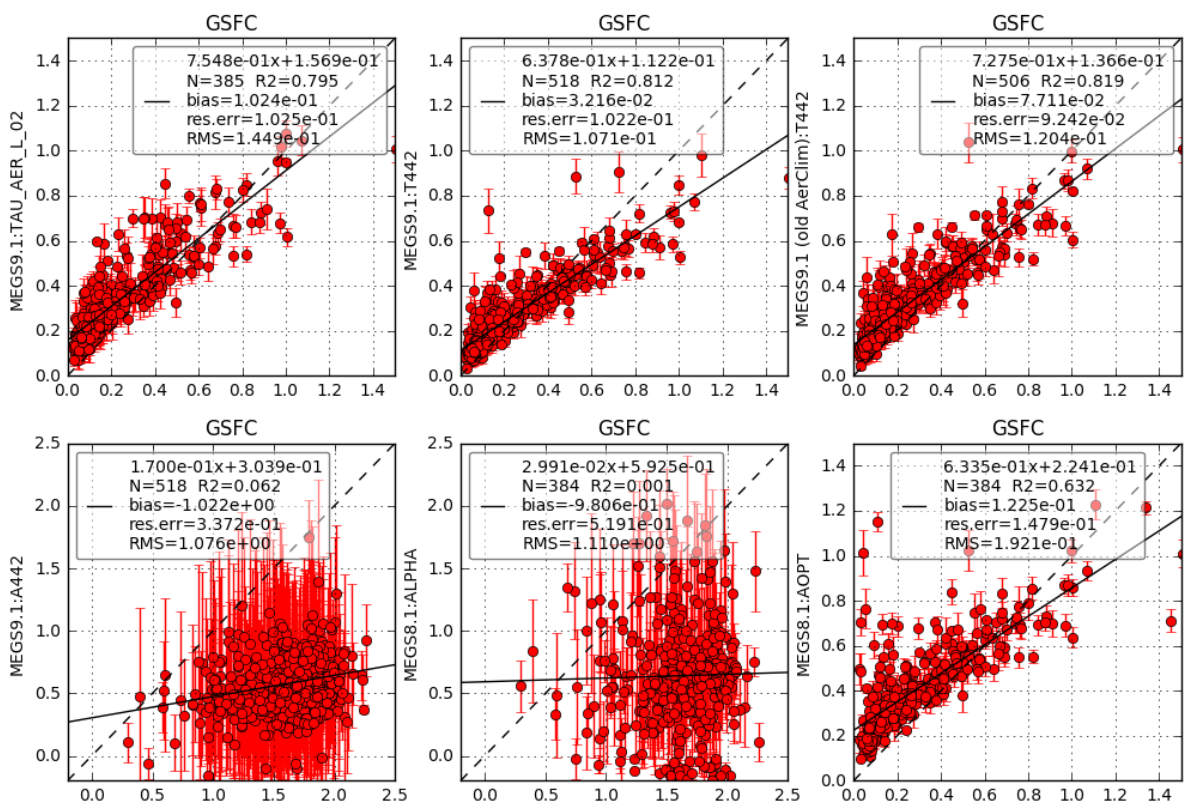

Figure 11: Matchups between 3rd and 4th RP products and Aeronet products for the GSFC site and the whole MERIS archive, error bars in th y xis correspond to the spatial standard deviation in 11x11 RR pixels boxes around the Aeronet site

The same analysis for the sites: 'AltaFloresta', 'Banizoumbou', 'Beijing', 'Dakar','Evora', 'GSFC', 'Ispra', 'Kanpur', 'Lille' is given in Annex 8

4.2 Validation against MODIS Monthly L3 products

For 4 months of 2008, (March, June, September and December), we compare the 3rd and 4th RP monthly L3 AOT with the MODIS monthly MYD08_M3 products, Collection 6.

Among the numerous MODIS output quantities we selected the 'Aerosol_Optical_Depth_Land_Mean_Mean'. MERIS and MODIS AOT's are given for 550 nm. MERIS products is also shown for ocean whereas MODIS is computed only for land.

MERIS Level 3 products was computed with compositng rules given in Annex 9

The main selection rule is to exlude the the morphologically dilated (by 10 pixels) (CLOUD OR CLOUD_AMBIGUOUS) mask.

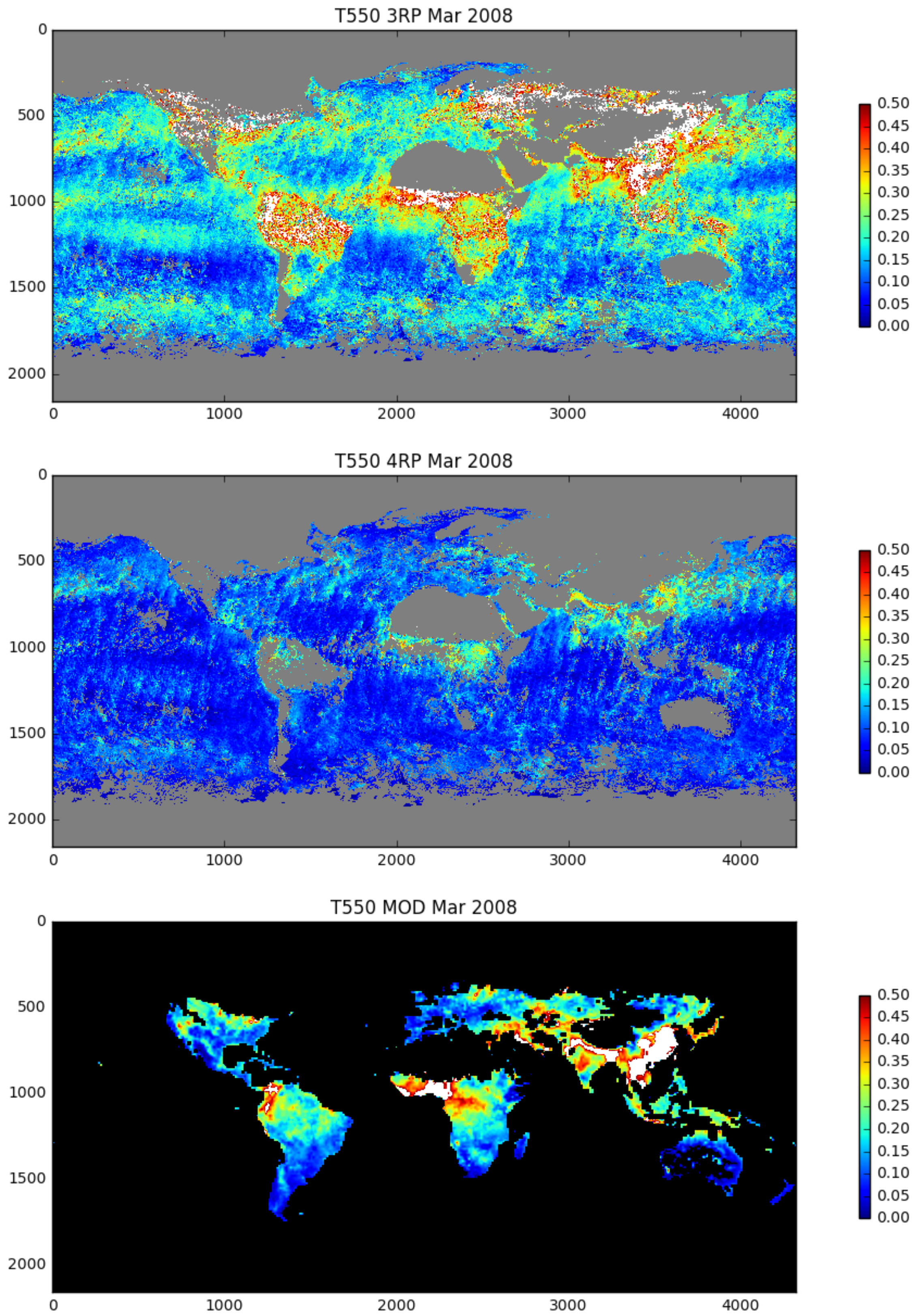

Figure 12: Monthly L3 products from 3rd and 4th RP along with MODIS MYD_08_M3 AOT at 550 nm for the month of March 2008

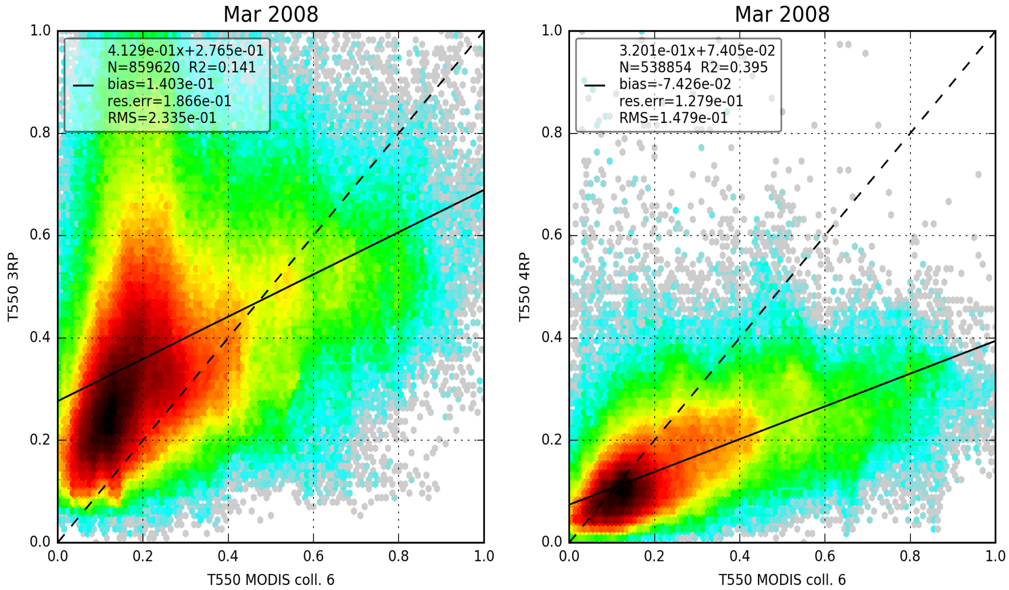

Figure 13: Regression between Monthly L3 products from 3rd and 4th RP along with MODIS MYD_08_M3 AOT at 550 nm for the month of March 2008

5 Annex : Verification of LARS surface reflectance model around Aeronet sites

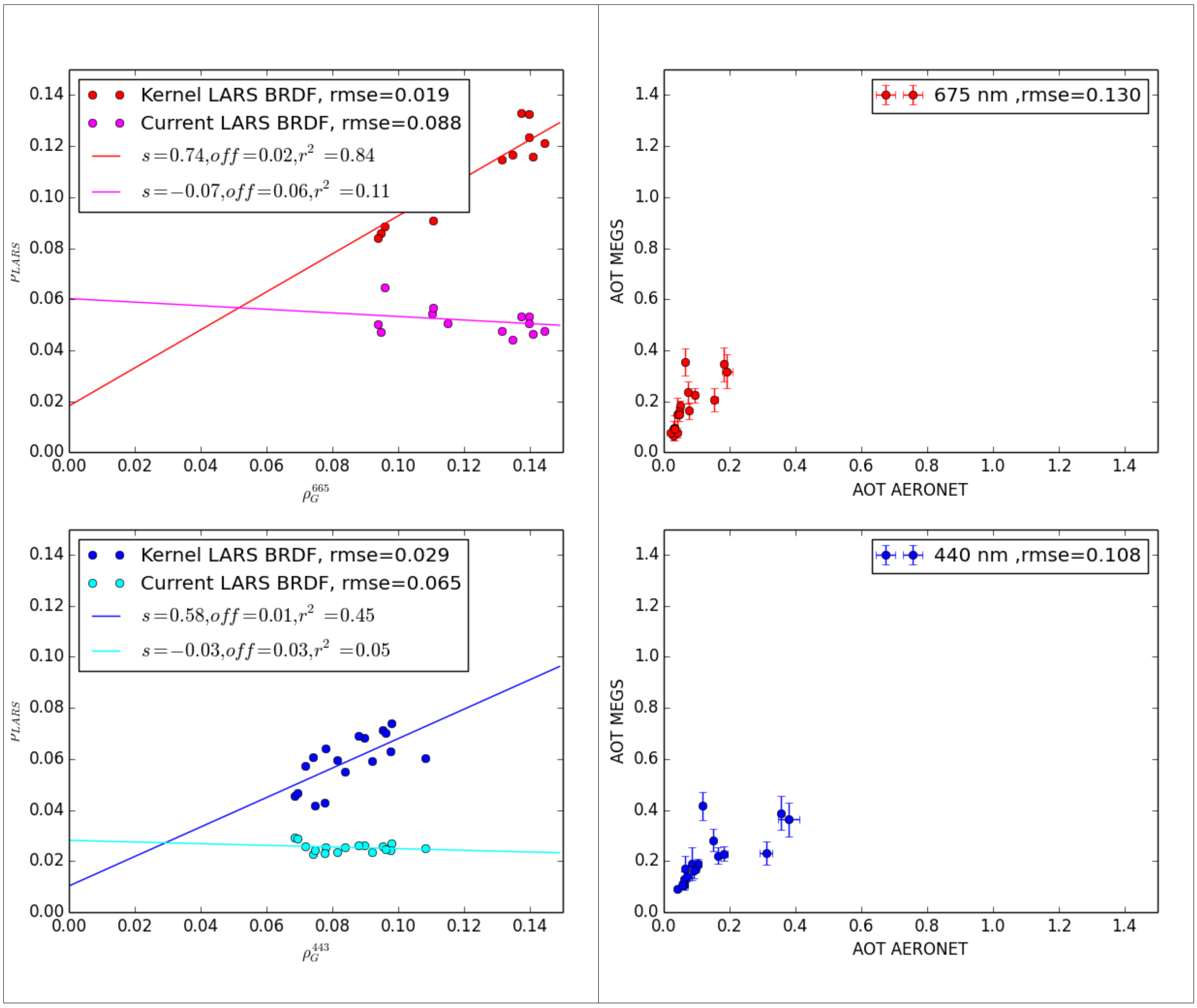

Figure 14: Same as Fig. 9 but for Barcelona (41N,2E)

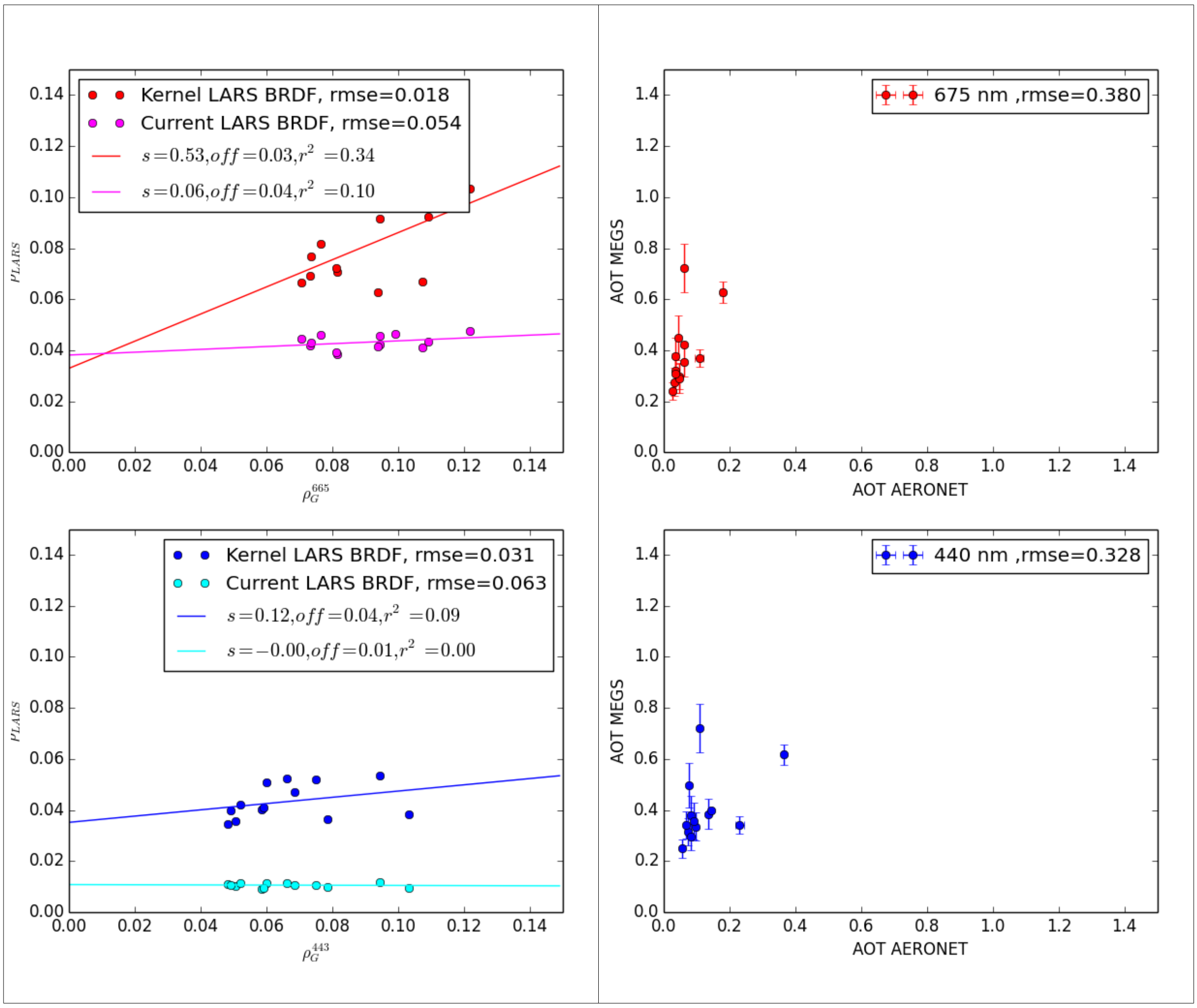

Figure 15: Same as Fig.9 but for Missoula (46N,117W)

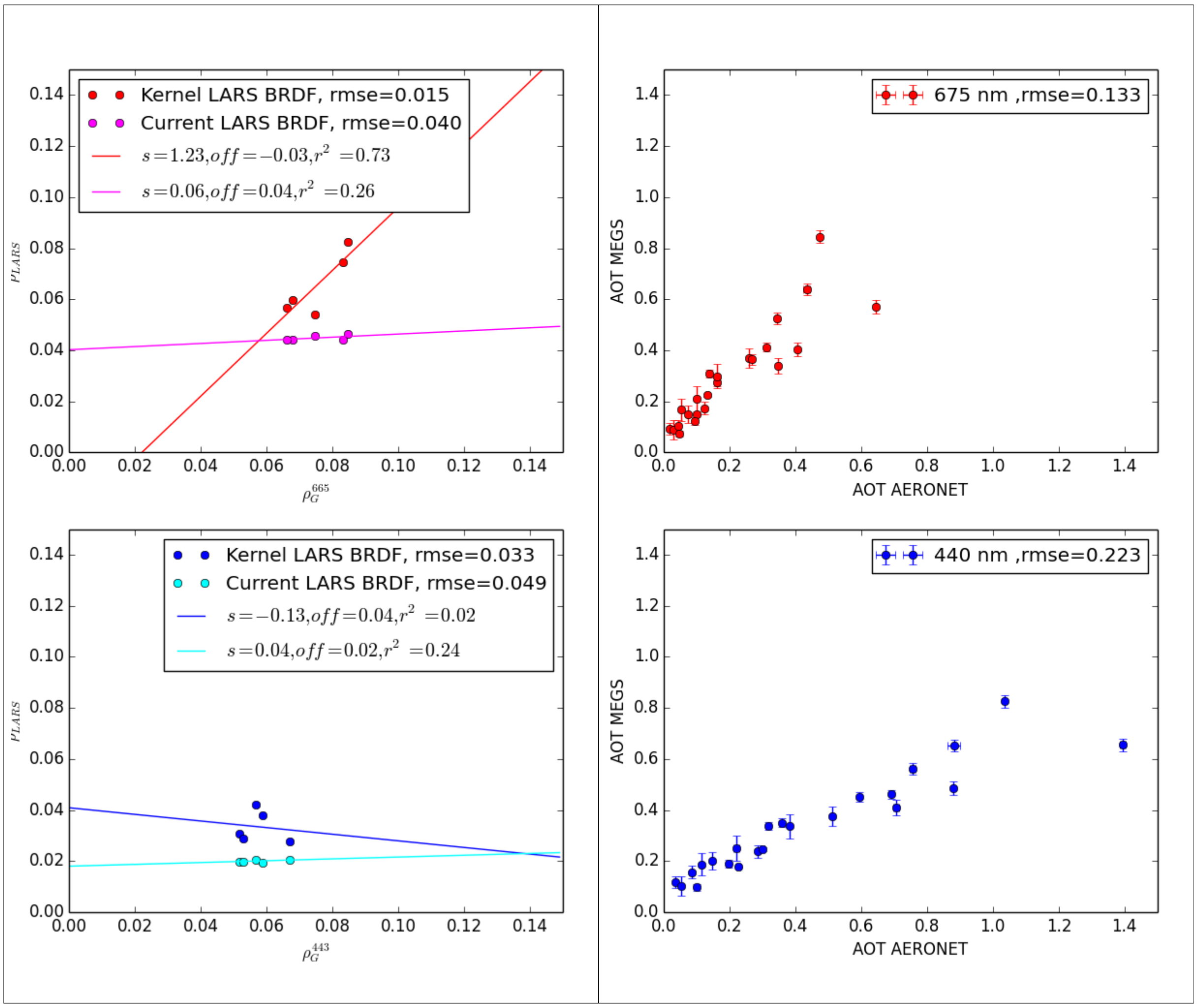

Figure 16: Same as Fig.9 but for Mongu (15S,23E)

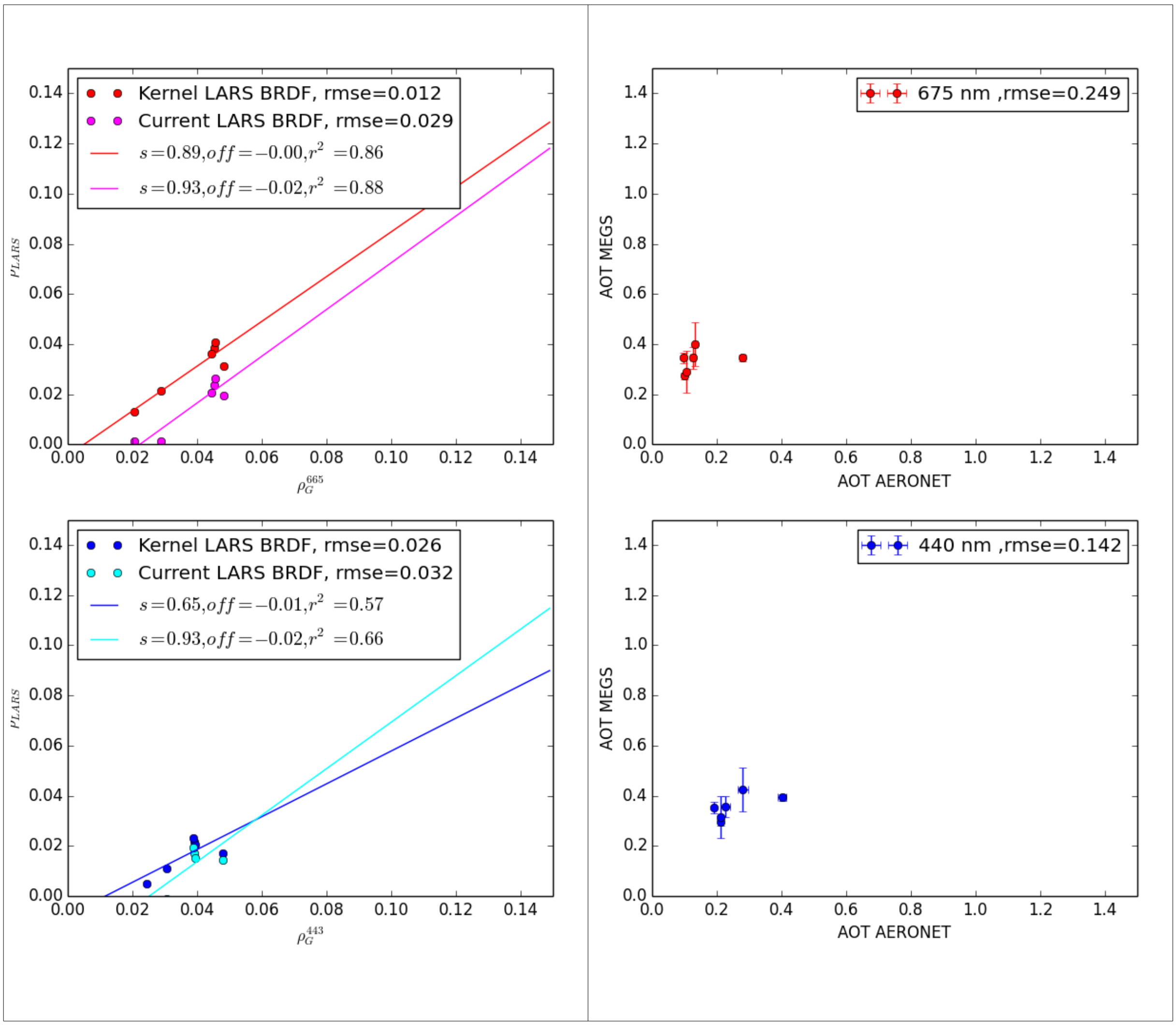

Figure 17: Same as Fig. 9 but for Noto (37N,137E)

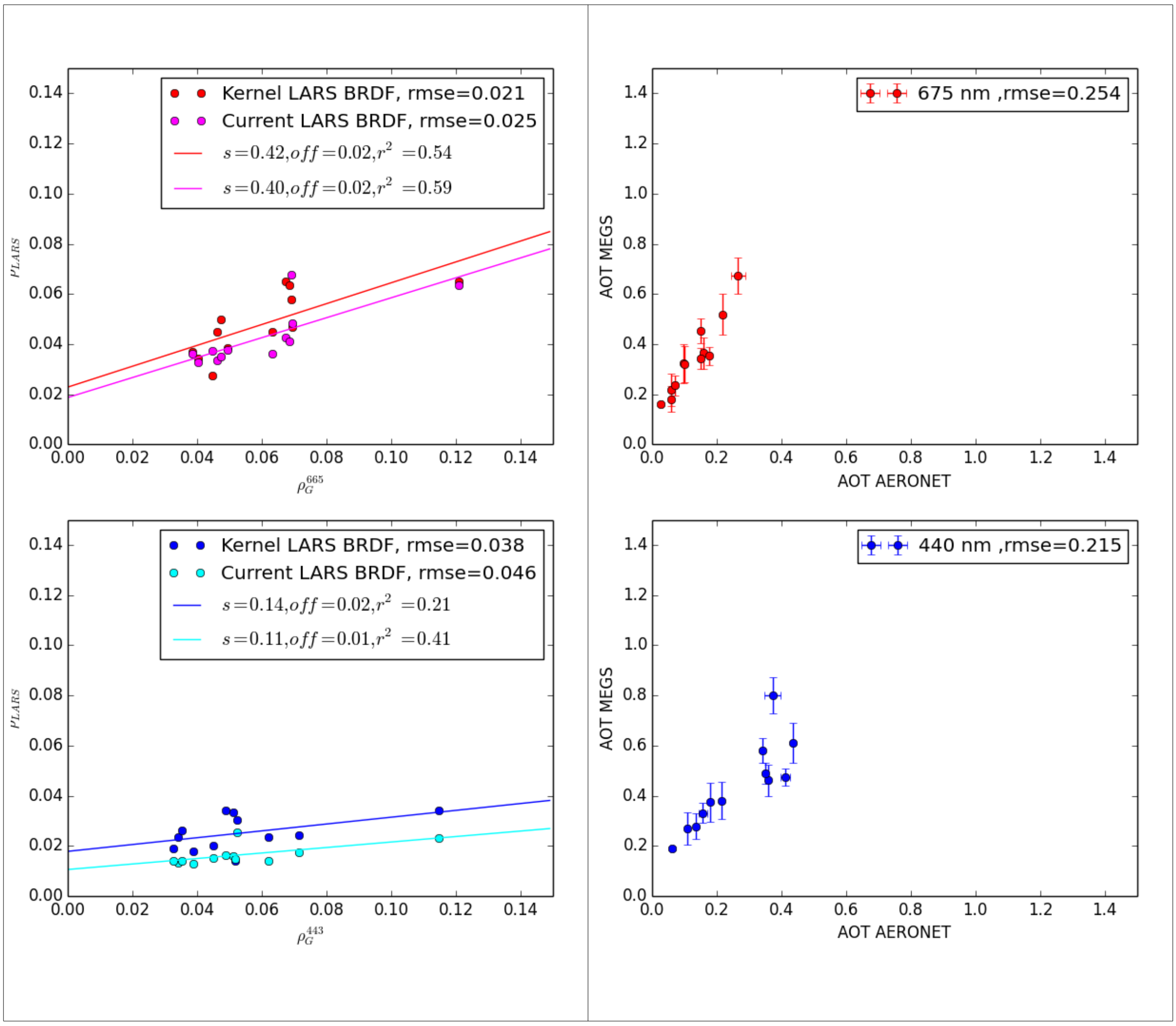

Figure 18: Same as Fig.9 but for GSFC (38N,76W)

6 Annex: Examples of LARS BRDF

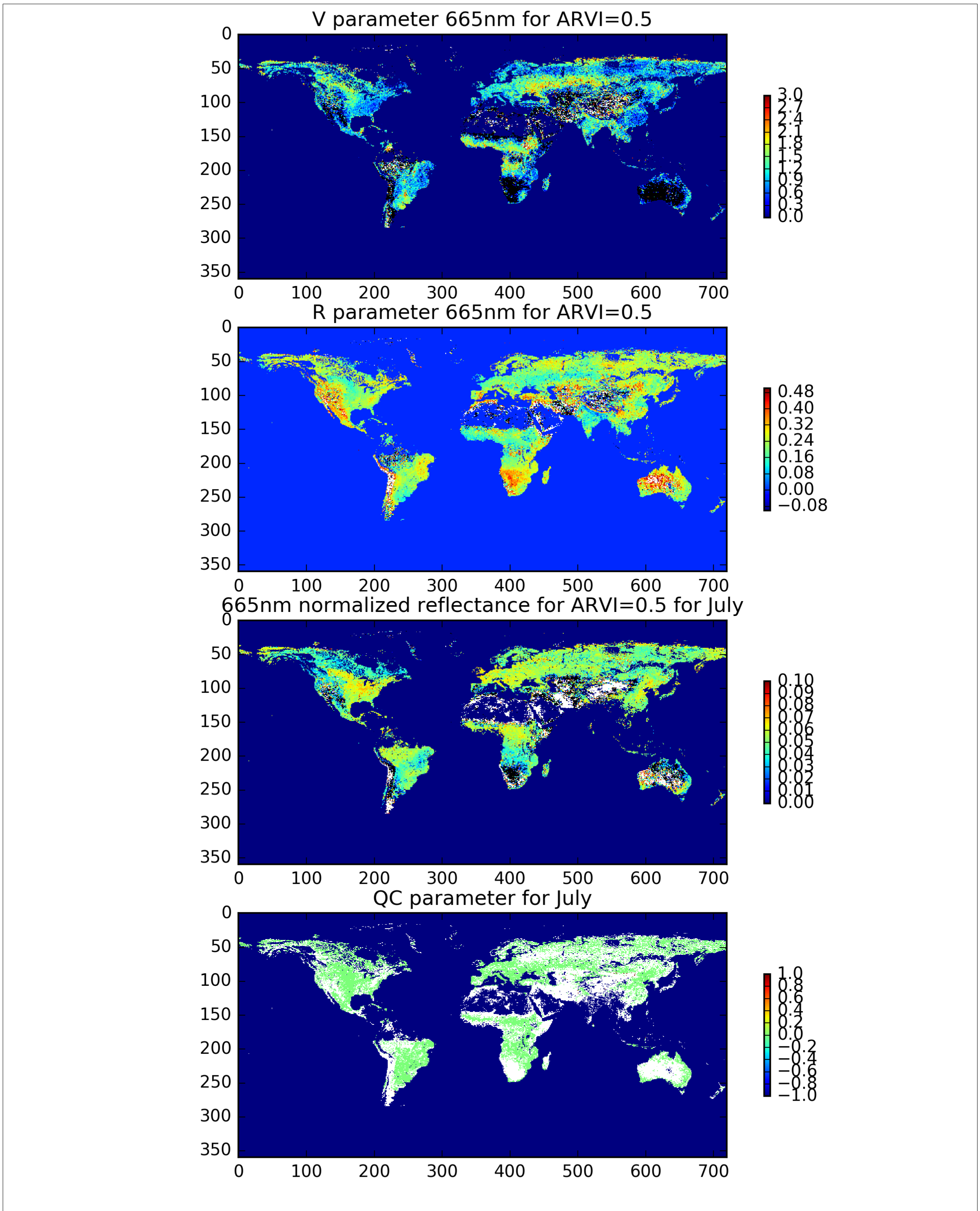

Figure 19: BRDF parameters of LARS from the Look up Tables computed for target of ARVI=0.5 and the month of July. The last map shows the quality index computed during the LUT making. The nominal quality index is 0. Negative values mean no data and values above zero mean degraded quality.

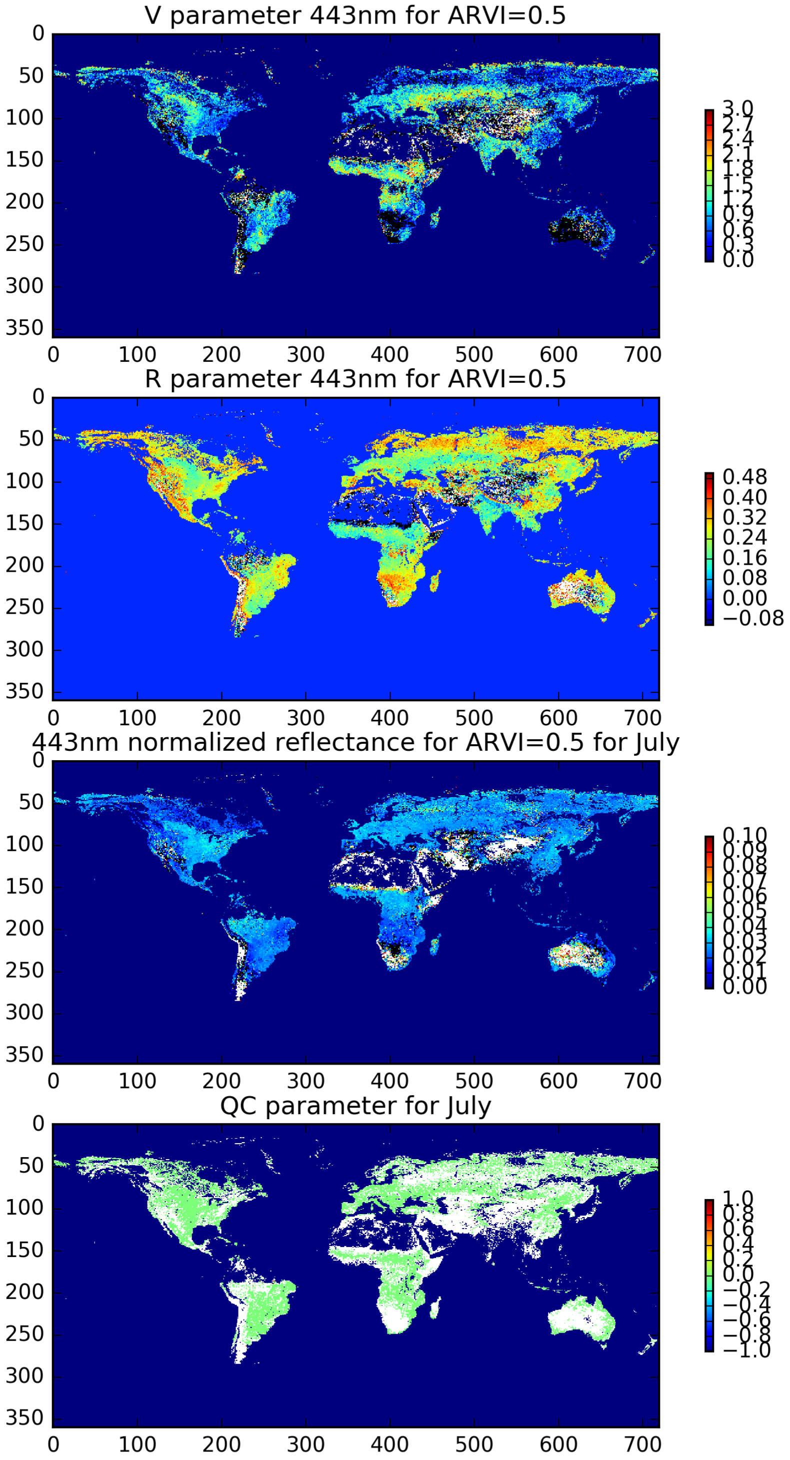

Figure 20: Same as Figure 19 but for 443 nm

7 Annex: Validation of AOT against MODIS L3 data and comparison between 3rd and 4th RP

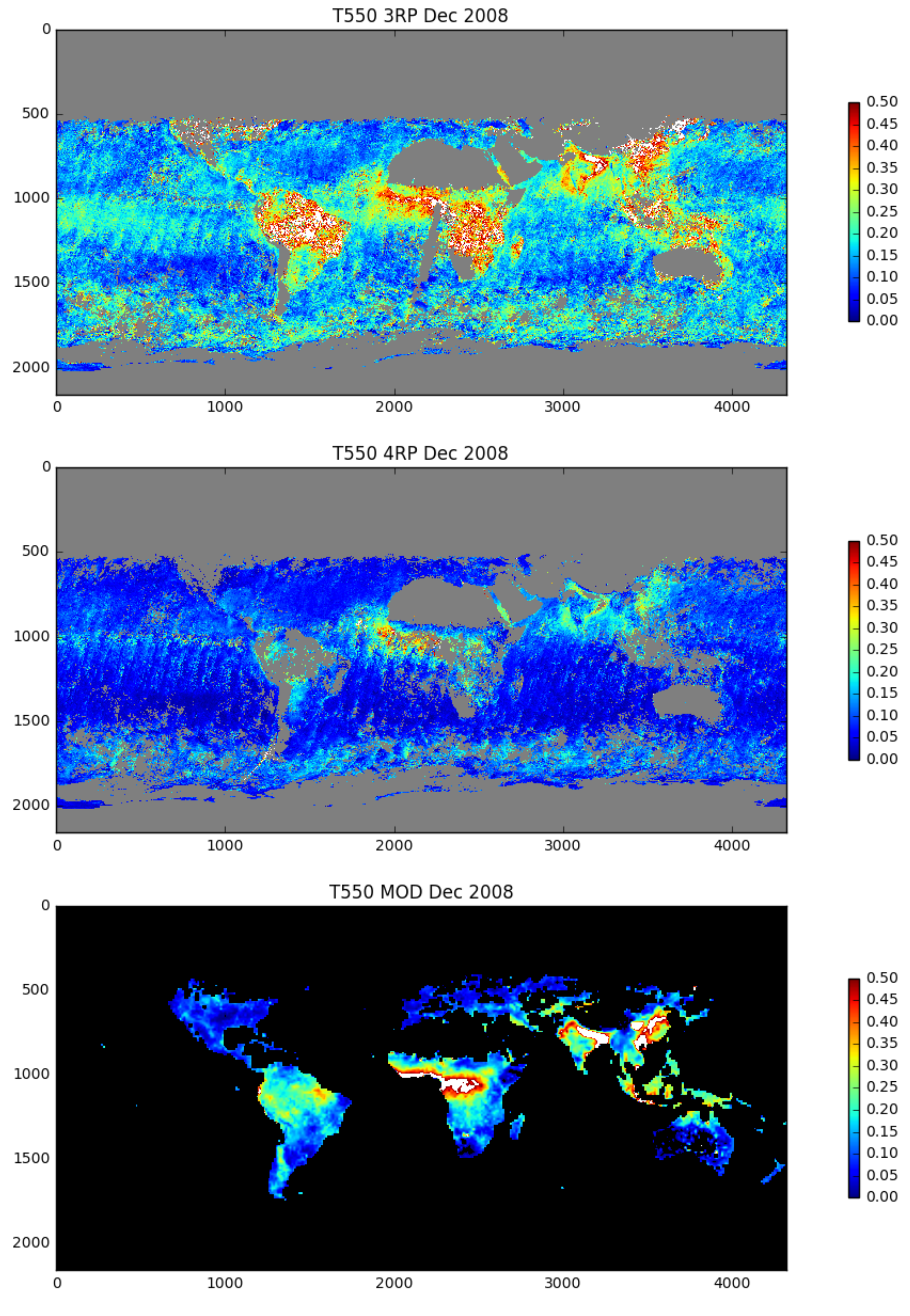
T550 3RP Dec 2008
T550 4RP Dec 2008
T550 MOD Dec 2008
0
500
1000
1500
2000
0
1000
2000
3000
4000
0.50
0.45
0.40
0.35
0.30
0.25
0.20
0.15
0.10
0.05
0.00

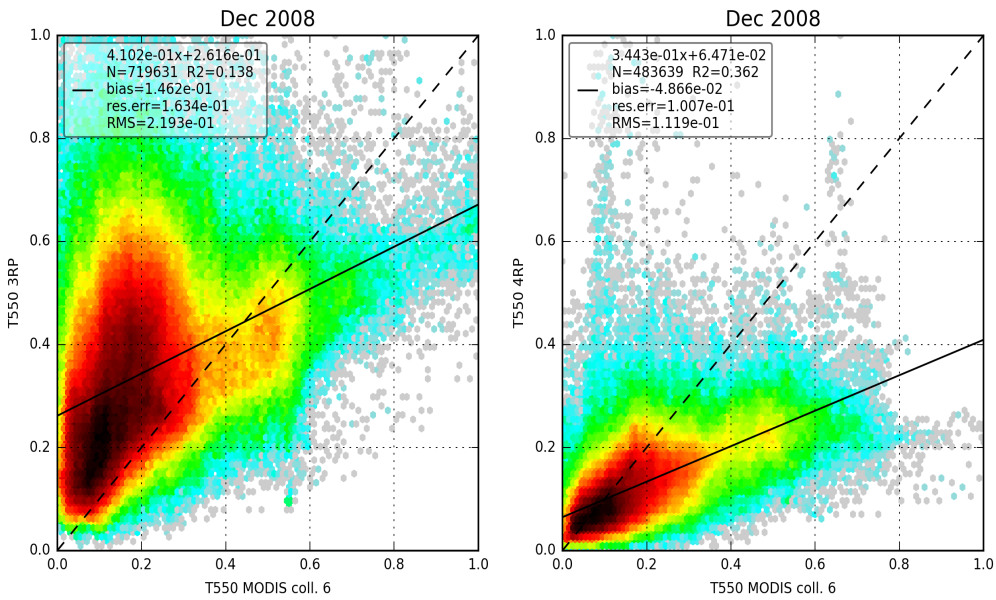
Dec 2008
4.102e-01x+2.616e-01
N=719631 R2=0.138
bias=1.462e-01
res.err=1.634e-01
RMS=2.193e-01
T550 3RP
T550 MODIS coll. 6
Dec 2008
3.443e-01x+6.471e-02
N=483639 R2=0.362
bias=-4.866e-02
res.err=1.007e-01
RMS=1.119e-01
T550 4RP
T550 MODIS coll. 6

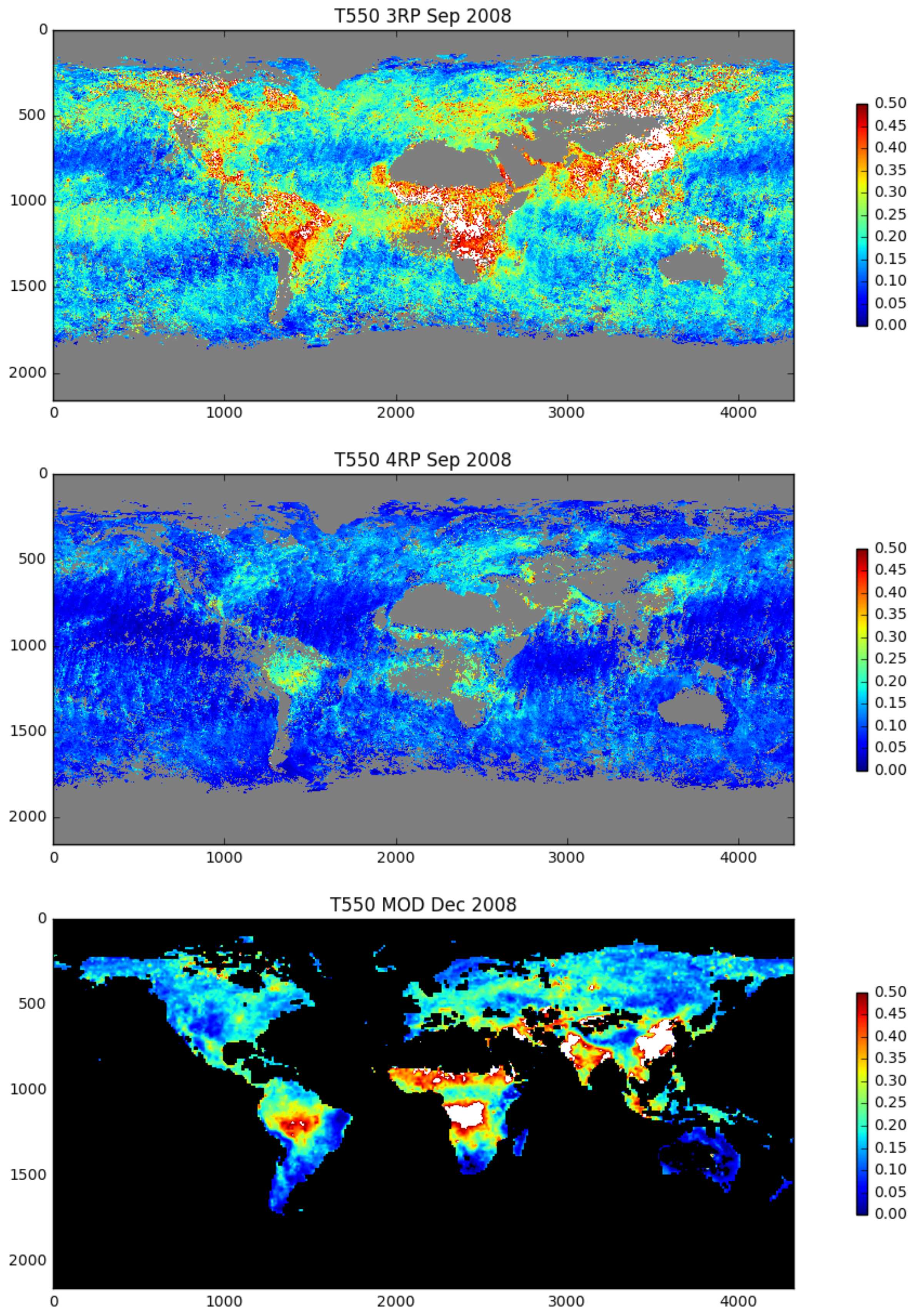
T550 3RP Sep 2008
T550 4RP Sep 2008
T550 MOD Dec 2008
0
500
1000
1500
2000
0
1000
2000
3000
4000
0.50
0.45
0.40
0.35
0.30
0.25
0.20
0.15
0.10
0.05
0.00

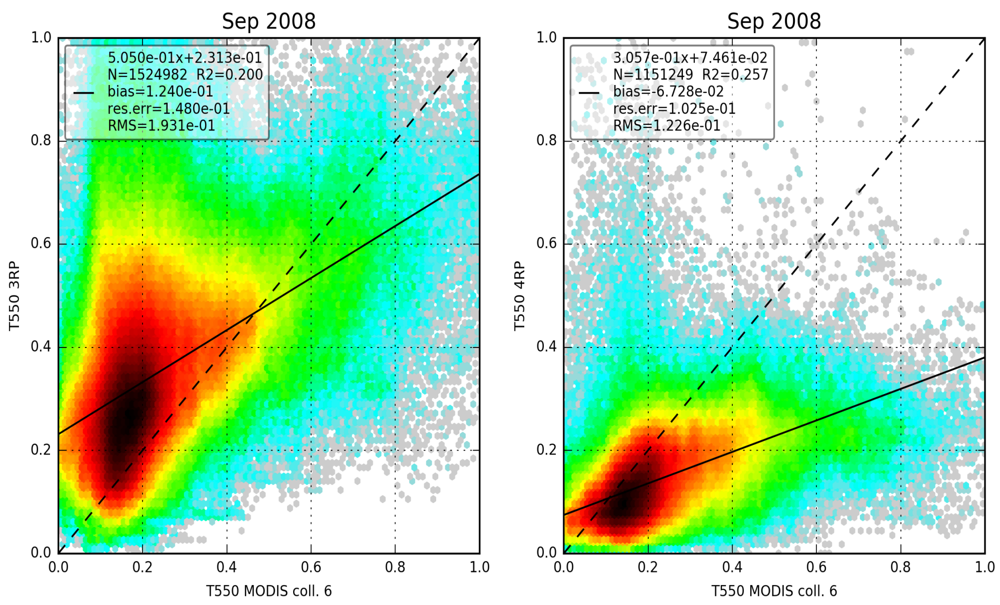
Sep 2008
5.050e-01x+2.313e-01
N=1524982 R2=0.200
bias=1.240e-01
res.err=1.480e-01
RMS=1.931e-01
T550 3RP
T550 MODIS coll. 6
Sep 2008
3.057e-01x+7.461e-02
N=1151249 R2=0.257
bias=-6.728e-02
res.err=1.025e-01
RMS=1.226e-01
T550 4RP
T550 MODIS coll. 6

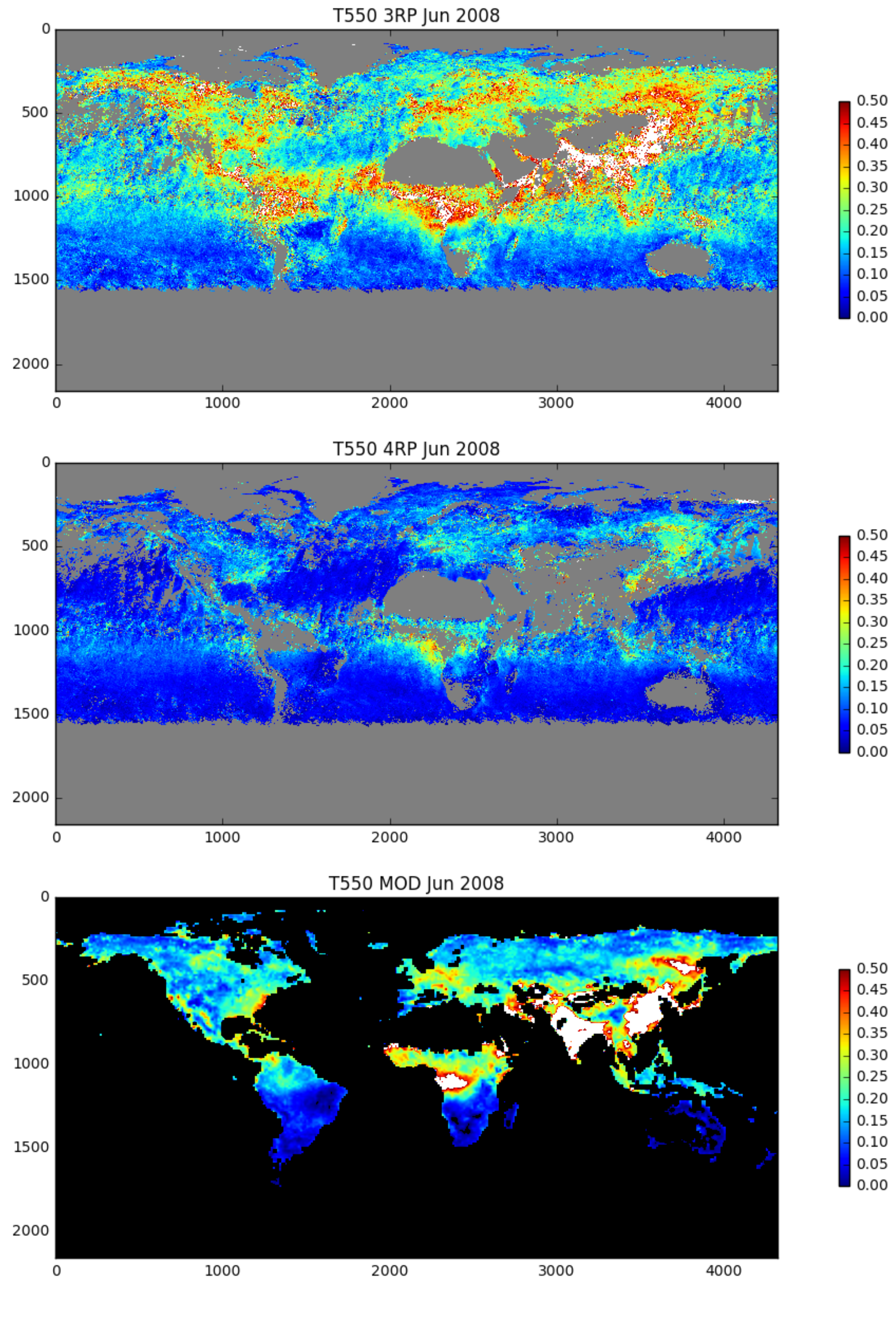

T550 3RP Jun 2008
T550 4RP Jun 2008
T550 MOD Jun 2008
0
500
1000
1500
2000
0
1000
2000
3000
4000
0.50
0.45
0.40
0.35
0.30
0.25
0.20
0.15
0.10
0.05
0.00

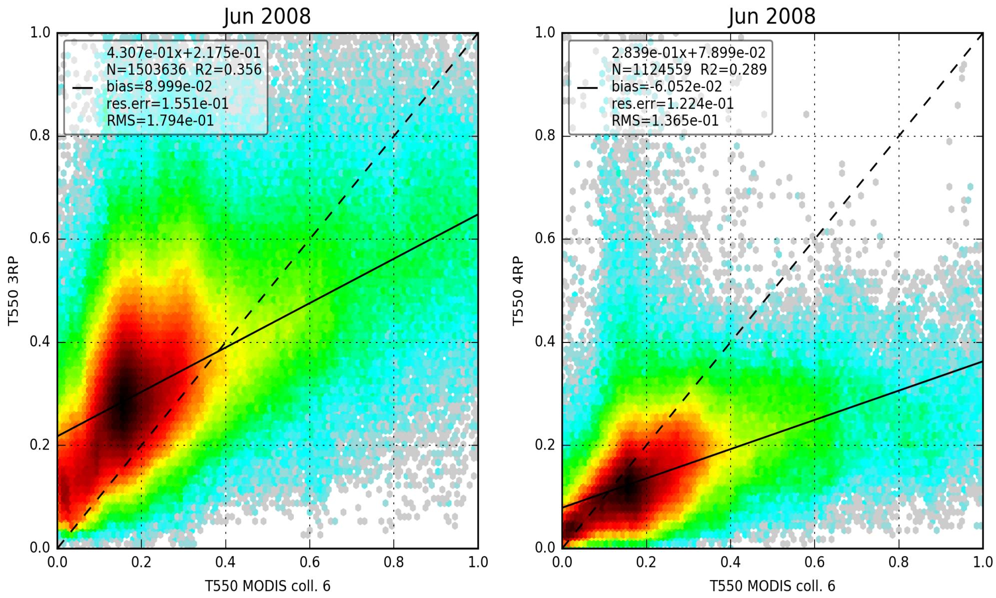
Jun 2008
4.307e-01x+2.175e-01
N=1503636 R2=0.356
bias=8.999e-02
res.err=1.551e-01
RMS=1.794e-01
T550 3RP
T550 MODIS coll. 6
Jun 2008
2.839e-01x+7.899e-02
N=1124559 R2=0.289
bias=-6.052e-02
res.err=1.224e-01
RMS=1.365e-01
T550 4RP
T550 MODIS coll. 6

8 Annex : Matchups against AERONET data

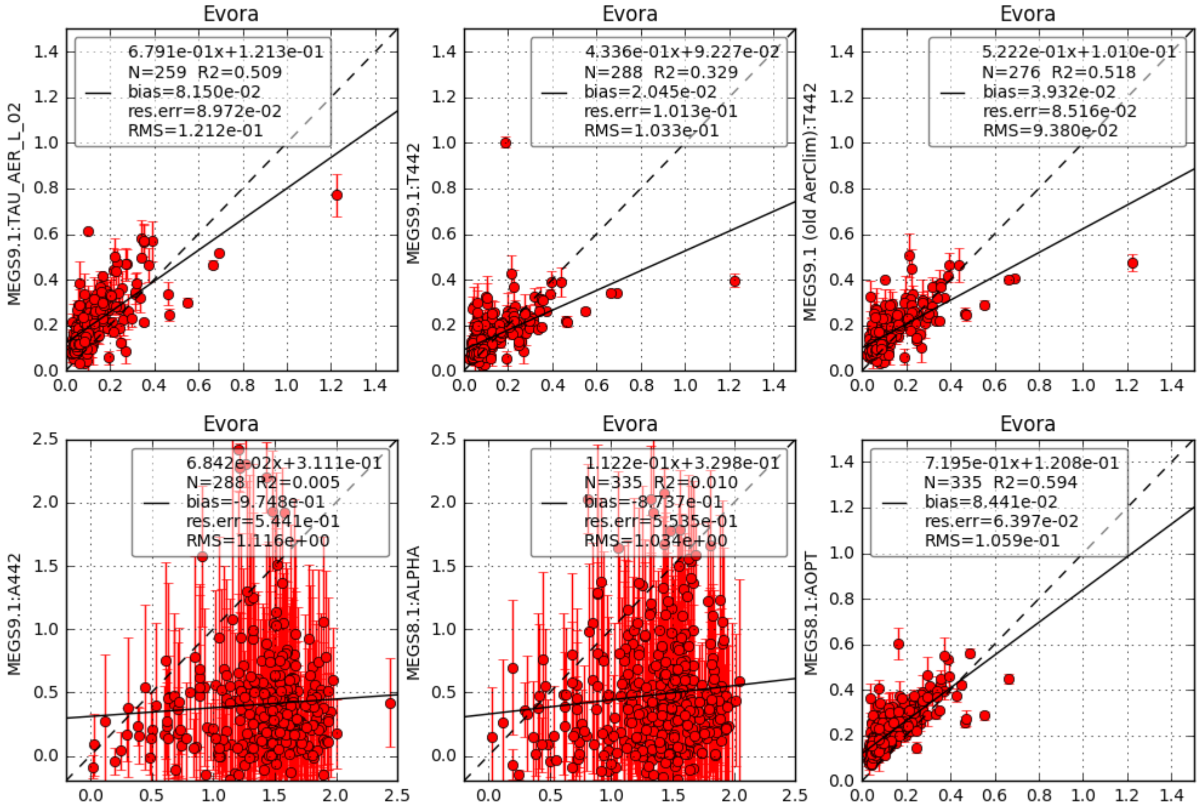

Evora
6.791e-01x+1.213e-01
N=259 R2=0.509
bias=8.150e-02
res.err=8.972e-02
RMS=1.212e-01
MEGS9.1:TAU_AER_L_02
Evora
4.336e-01x+9.227e-02
N=288 R2=0.329
bias=2.045e-02
res.err=1.013e-01
RMS=1.033e-01
MEGS9.1:T442
Evora
5.222e-01x+1.010e-01
N=276 R2=0.518
bias=3.932e-02
res.err=8.516e-02
RMS=9.380e-02
MEGS9.1 (old AerClim):T442
Evora
6.842e-02x+3.111e-01
N=288 R2=0.005
bias=-9.748e-01
res.err=5.441e-01
RMS=1.116e+00
MEGS9.1:A442
Evora
1.122e-01x+3.298e-01
N=335 R2=0.010
bias=-8.737e-01
res.err=5.535e-01
RMS=1.034e+00
MEGS8.1:ALPHA
Evora
7.195e-01x+1.208e-01
N=335 R2=0.594
bias=8.441e-02
res.err=6.397e-02
RMS=1.059e-01
MEGS8.1:AOPT

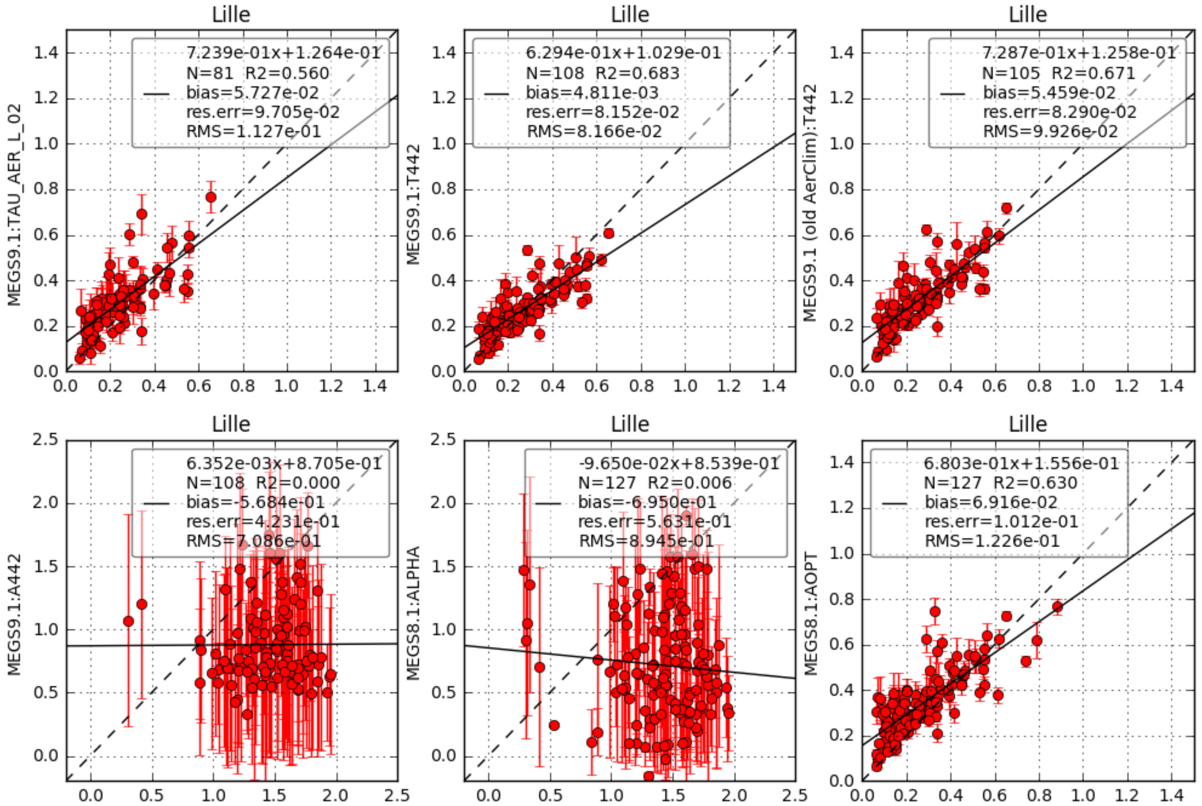

Lille
7.239e-01x+1.264e-01
N=81 R2=0.560
bias=5.727e-02
res.err=9.705e-02
RMS=1.127e-01
MEGS9.1:TAU_AER_L_02
Lille
6.294e-01x+1.029e-01
N=108 R2=0.683
bias=4.811e-03
res.err=8.152e-02
RMS=8.166e-02
MEGS9.1:T442
Lille
7.287e-01x+1.258e-01
N=105 R2=0.671
bias=5.459e-02
res.err=8.290e-02
RMS=9.926e-02
MEGS9.1 (old AerClim):T442
Lille
6.352e-03x+8.705e-01
N=108 R2=0.000
bias=-5.684e-01
res.err=4.231e-01
RMS=7.086e-01
MEGS9.1:A442
Lille
-9.650e-02x+8.539e-01
N=127 R2=0.006
bias=-6.950e-01
res.err=5.631e-01
RMS=8.945e-01
MEGS8.1:ALPHA
Lille
6.803e-01x+1.556e-01
N=127 R2=0.630
bias=6.916e-02
res.err=1.012e-01
RMS=1.226e-01
MEGS8.1:AOPT

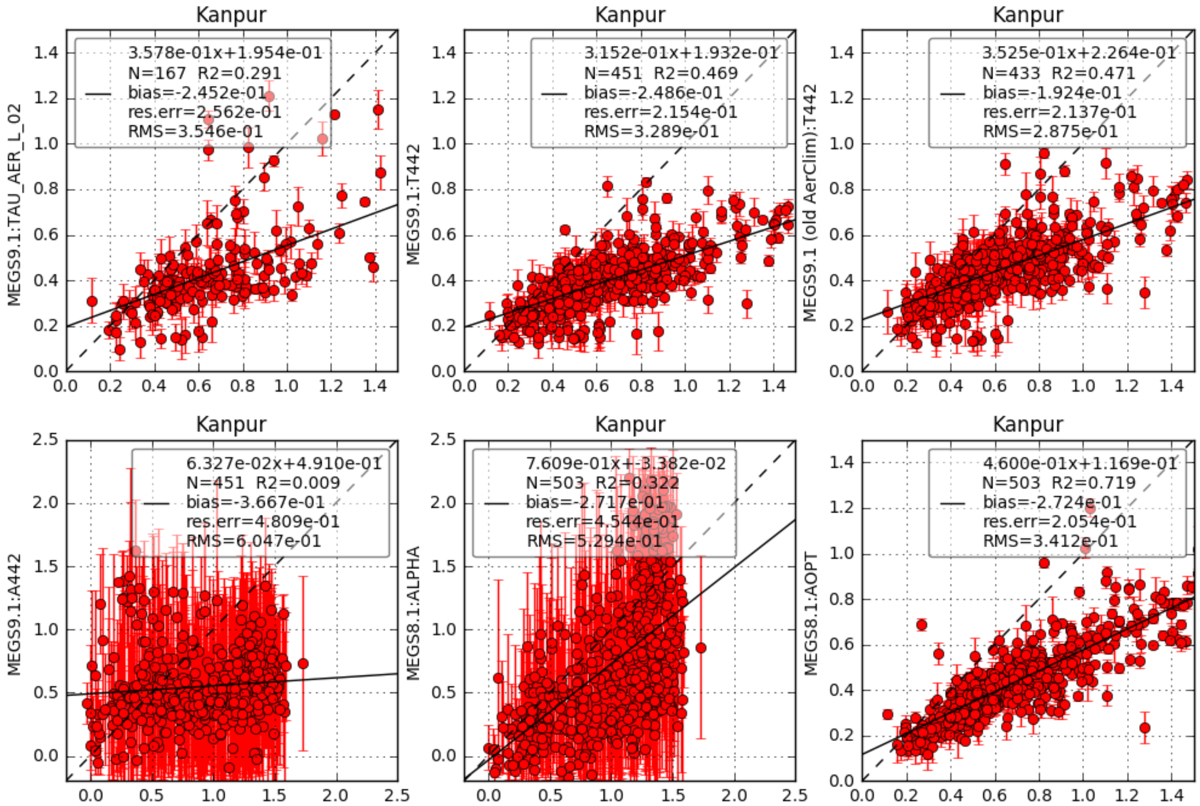
Kanpur
3.578e-01x+1.954e-01
N=167 R2=0.291
bias=-2.452e-01
res.err=2.562e-01
RMS=3.546e-01
MEGS9.1:TAU_AER_L_02
Kanpur
3.152e-01x+1.932e-01
N=451 R2=0.469
bias=-2.486e-01
res.err=2.154e-01
RMS=3.289e-01
MEGS9.1:T442
Kanpur
3.525e-01x+2.264e-01
N=433 R2=0.471
bias=-1.924e-01
res.err=2.137e-01
RMS=2.875e-01
MEGS9.1 (old AerClim):T442
Kanpur
6.327e-02x+4.910e-01
N=451 R2=0.009
bias=-3.667e-01
res.err=4.809e-01
RMS=6.047e-01
MEGS9.1:A442
Kanpur
7.609e-01x+-3.382e-02
N=503 R2=0.322
bias=-2.717e-01
res.err=4.544e-01
RMS=5.294e-01
MEGS8.1:ALPHA
Kanpur
4.600e-01x+1.169e-01
N=503 R2=0.719
bias=-2.724e-01
res.err=2.054e-01
RMS=3.412e-01
MEGS8.1:AOPT

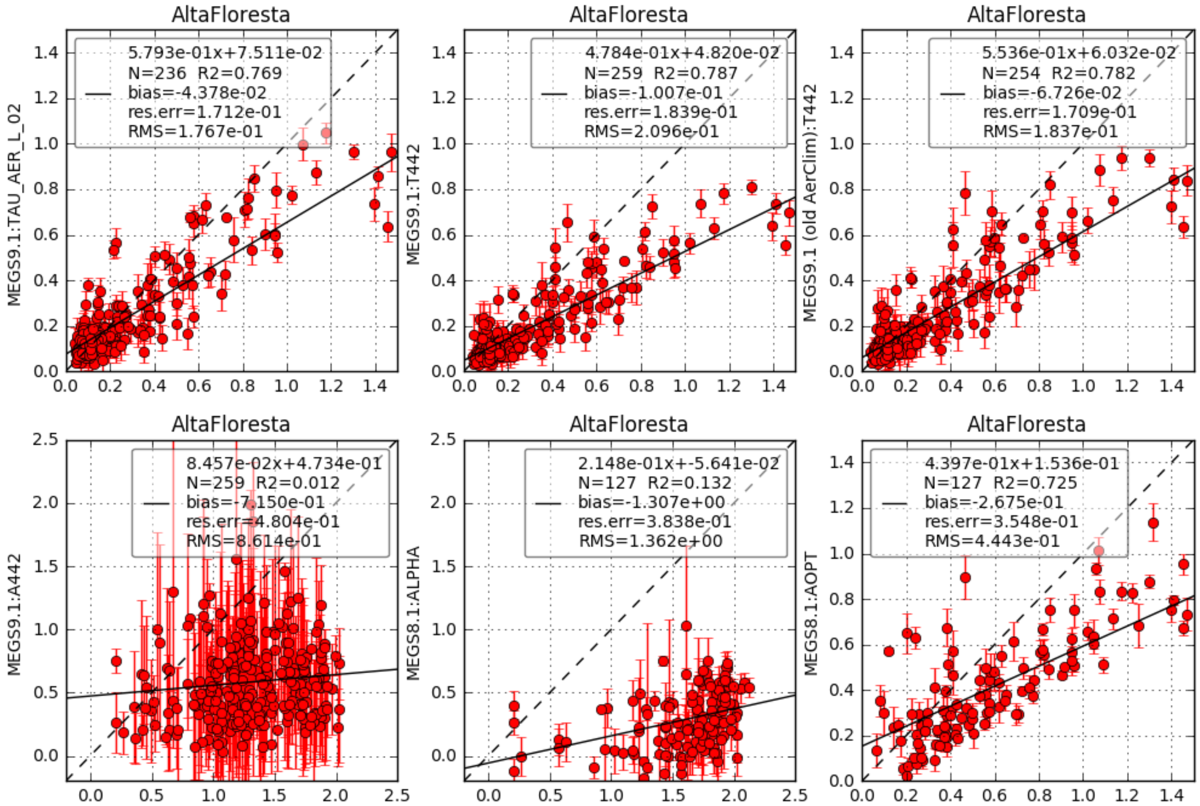

AltaFloresta
5.793e-01x+7.511e-02
N=236 R2=0.769
bias=-4.378e-02
res.err=1.712e-01
RMS=1.767e-01
MEGS9.1:TAU_AER_L_02
AltaFloresta
4.784e-01x+4.820e-02
N=259 R2=0.787
bias=-1.007e-01
res.err=1.839e-01
RMS=2.096e-01
MEGS9.1:T442
AltaFloresta
5.536e-01x+6.032e-02
N=254 R2=0.782
bias=-6.726e-02
res.err=1.709e-01
RMS=1.837e-01
MEGS9.1 (old AerClim):T442
AltaFloresta
8.457e-02x+4.734e-01
N=259 R2=0.012
bias=-7.150e-01
res.err=4.804e-01
RMS=8.614e-01
MEGS9.1:A442
AltaFloresta
2.148e-01x+-5.641e-02
N=127 R2=0.132
bias=-1.307e+00
res.err=3.838e-01
RMS=1.362e+00
MEGS8.1:ALPHA
AltaFloresta
4.397e-01x+1.536e-01
N=127 R2=0.725
bias=-2.675e-01
res.err=3.548e-01
RMS=4.443e-01
MEGS8.1:AOPT

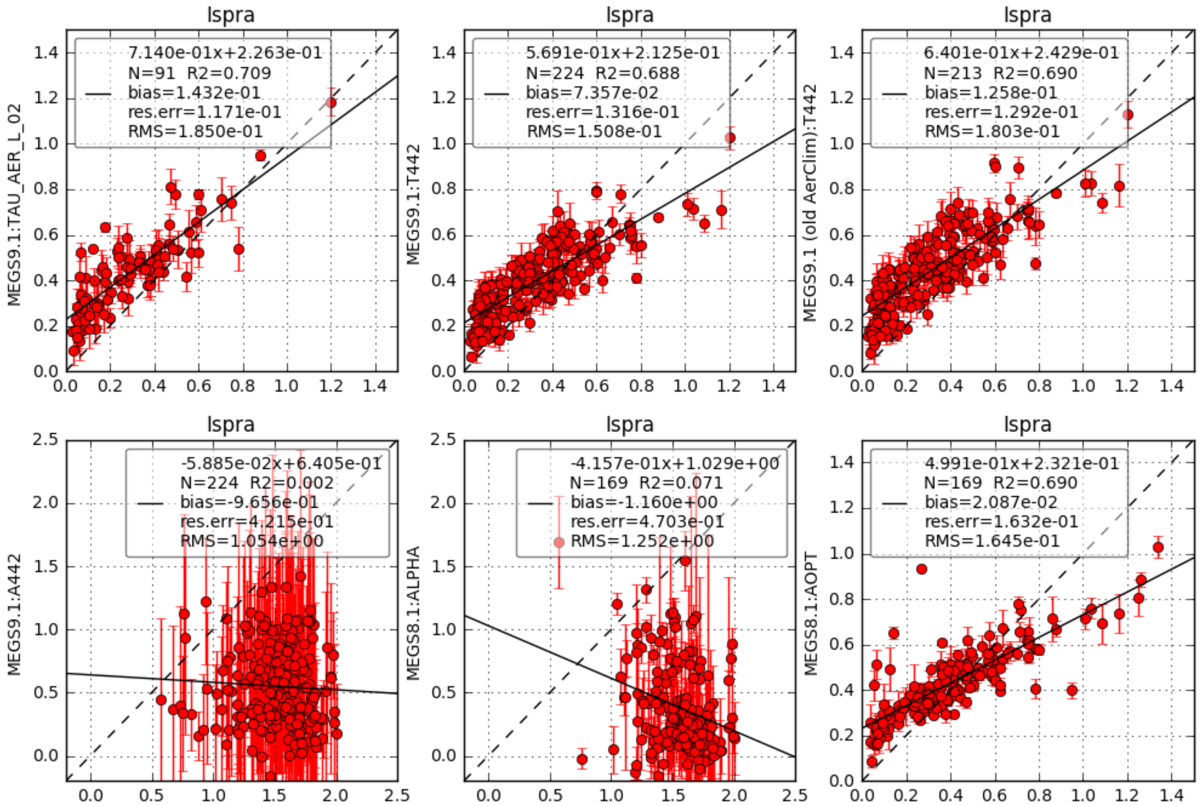

Ispra
7.140e-01x+2.263e-01
N=91 R2=0.709
bias=1.432e-01
res.err=1.171e-01
RMS=1.850e-01
MEGS9.1:TAU_AER_L_02
Ispra
5.691e-01x+2.125e-01
N=224 R2=0.688
bias=7.357e-02
res.err=1.316e-01
RMS=1.508e-01
MEGS9.1:T442
Ispra
6.401e-01x+2.429e-01
N=213 R2=0.690
bias=1.258e-01
res.err=1.292e-01
RMS=1.803e-01
MEGS9.1 (old AerClim):T442
Ispra
-5.885e-02x+6.405e-01
N=224 R2=0.002
bias=-9.656e-01
res.err=4.215e-01
RMS=1.054e+00
MEGS9.1:A442
Ispra
-4.157e-01x+1.029e+00
N=169 R2=0.071
bias=-1.160e+00
res.err=4.703e-01
RMS=1.252e+00
MEGS8.1:ALPHA
Ispra
4.991e-01x+2.321e-01
N=169 R2=0.690
bias=2.087e-02
res.err=1.632e-01
RMS=1.645e-01
MEGS8.1:AOPT

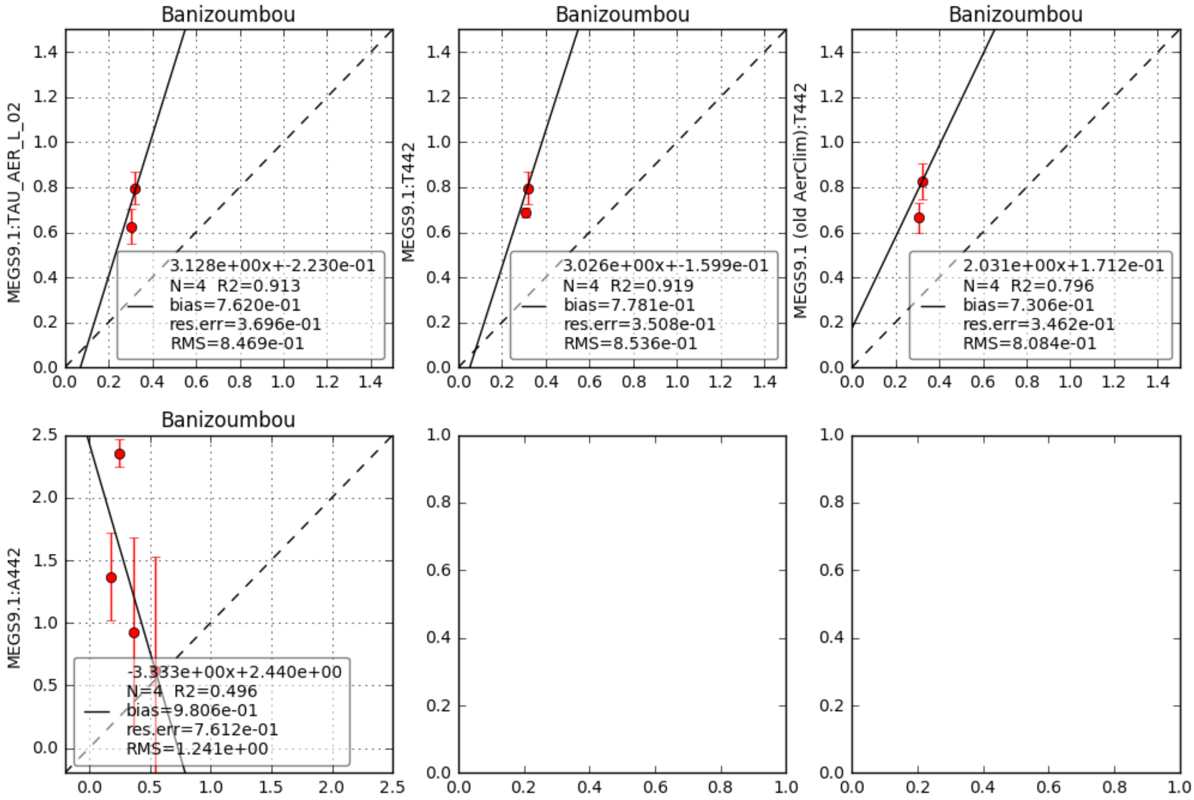

Banizoumbou
MEGS9.1:TAU_AER_L_02
3.128e+00x+-2.230e-01
N=4 R2=0.913
bias=7.620e-01
res.err=3.696e-01
RMS=8.469e-01
Banizoumbou
MEGS9.1:T442
3.026e+00x+-1.599e-01
N=4 R2=0.919
bias=7.781e-01
res.err=3.508e-01
RMS=8.536e-01
Banizoumbou
MEGS9.1 (old AerClim):T442
2.031e+00x+1.712e-01
N=4 R2=0.796
bias=7.306e-01
res.err=3.462e-01
RMS=8.084e-01
Banizoumbou
MEGS9.1:A442
-3.333e+00x+2.440e+00
N=4 R2=0.496
bias=9.806e-01
res.err=7.612e-01
RMS=1.241e+00

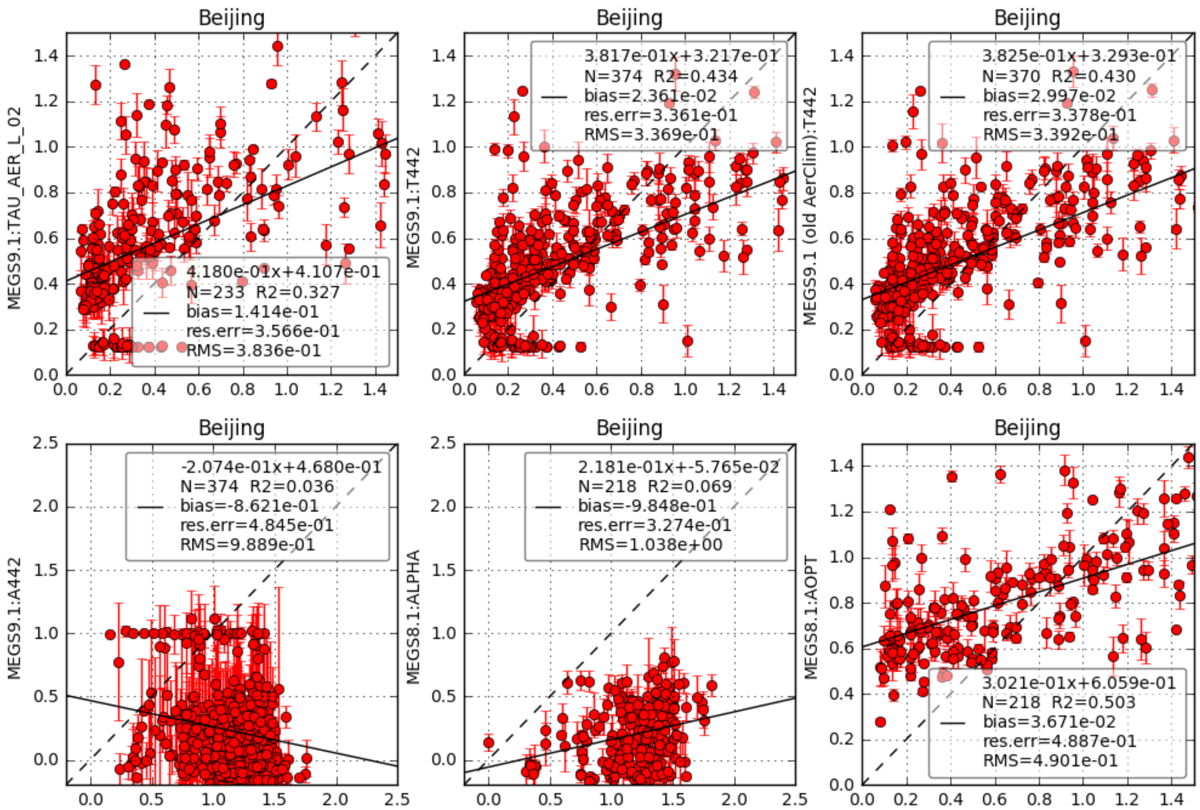

Beijing
MEGS9.1:TAU_AER_L_02
4.180e-01x+4.107e-01
N=233 R2=0.327
bias=1.414e-01
res.err=3.566e-01
RMS=3.836e-01
Beijing
MEGS9.1:T442
3.817e-01x+3.217e-01
N=374 R2=0.434
bias=2.361e-02
res.err=3.361e-01
RMS=3.369e-01
Beijing
MEGS9.1 (old AerClim):T442
3.825e-01x+3.293e-01
N=370 R2=0.430
bias=2.997e-02
res.err=3.378e-01
RMS=3.392e-01
Beijing
MEGS9.1:A442
-2.074e-01x+4.680e-01
N=374 R2=0.036
bias=-8.621e-01
res.err=4.845e-01
RMS=9.889e-01
Beijing
MEGS8.1:ALPHA
2.181e-01x+-5.765e-02
N=218 R2=0.069
bias=-9.848e-01
res.err=3.274e-01
RMS=1.038e+00
Beijing
MEGS8.1:AOPT
3.021e-01x+6.059e-01
N=218 R2=0.503
bias=3.671e-02
res.err=4.887e-01
RMS=4.901e-01

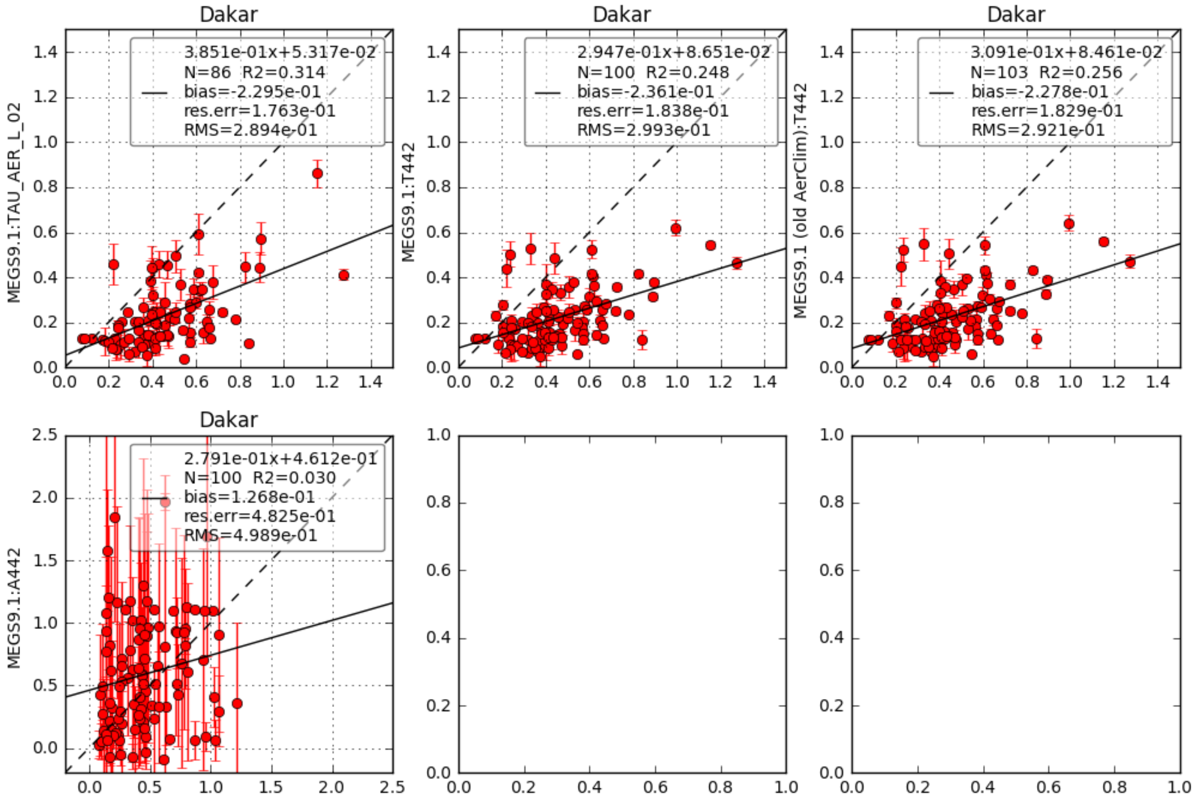

Dakar
3.851e-01x+5.317e-02
N=86 R2=0.314
bias=-2.295e-01
res.err=1.763e-01
RMS=2.894e-01
MEGS9.1:TAU_AER_L_02
Dakar
2.947e-01x+8.651e-02
N=100 R2=0.248
bias=-2.361e-01
res.err=1.838e-01
RMS=2.993e-01
MEGS9.1:T442
Dakar
3.091e-01x+8.461e-02
N=103 R2=0.256
bias=-2.278e-01
res.err=1.829e-01
RMS=2.921e-01
MEGS9.1 (old AerClim):T442
Dakar
2.791e-01x+4.612e-01
N=100 R2=0.030
bias=1.268e-01
res.err=4.825e-01
RMS=4.989e-01
MEGS9.1:A442

9 Annex : Compositing rules for the MERIS Level 3 4th RP

1) T442

Aerosol optical thickness over land at 442 nm with Aerosol model from the climatology

CO_DO_LAND
and not (LP_PC_{T}442_FAIL and **not F_T442**
or CLOUD_AMB_HAZE_enlarged**X1**)
and Q > **X2 and Note 4RP**

2) A443

Aerosol Angström Coefficient

CO_DO_LAND
and not (LP_PC_{T/A}442_FAIL and **not F_T442 and not F_A442**
or CLOUD_AMB_HAZE_enlarged**X1**)
and Q > X2 and Note 4RP

3) T443_ALPHA

Aerosol optical thickness over land at 442 nm with Aerosol model retrieved from the measurement

CO_DO_LAND
and not (LP_PC_{T/A}442_FAIL and **not F_T442 and not F_A442**
or CLOUD_AMB_HAZE_enlarged**X1**)
and Q > X2 and Note 4RP

Note 4RP

Apply a standard deviation filter on product P in (T442/A442/T442_ALPHA) on a 9x9 box: discard the pixel if it is not in
[mean - max(2*stddev, **scale**), mean + max(2*stddev, **scale**)], with mean and stddev computed using all P valid pixels. The term max(2*stddev, **scale**) allows to handle homogeneous areas (we don't want discard all pixels if stddev is very small).

On the remaining pixels average and compute stdev again in 9x9 boxes. Discard all pixels in the box if stdev> **X3**

Free parameters

X1 : 10 pixels
X2 : 0
X3 : (0.1, 0.5, 0.1) for P in (T443/A443/T443_ALPHA)
scale : (0.02, 0.1,0.02) for P in (T443/A443/T443_ALPHA)